AD NUMBER: AD0812993
LIMITATION CHANGES
TO: Approved for public release; distribution is unlimited.
FROM: This document is subject to special export controls and each transmittal to foreign governments or foreign nationals may be made only with prior approval of AFFDL (FDD), Wright-Patterson Air Force Base, Ohio 45433.
AUTHORITY
ST-A AFWAL LTR, 7 MAY 1976

AFFDL-TR-66-196

MICROPHONE SYSTEM FOR THE MEASUREMENT OF BOUNDARY LAYER PRESSURE FLUCTUATIONS

J. C. ORTEGA

WESTERN ELECTRIC-ACOUSTIC LABORATORY, INC.
LOS ANGELES, CALIFORNIA

TECHNICAL REPORT AFFDL-TR-66-196

JANUARY 1967

AIR FORCE FLIGHT DYNAMICS LABORATORY
RESEARCH AND TECHNOLOGY DIVISION
AIR FORCE SYSTEMS COMMAND
WRIGHT-PATTERSON AIR FORCE BASE, OHIO

NOTICES

When Government drawings, specifications, or other data are used for any purpose other than in connection with a definitely related Government procurement operation, the United States Government thereby incurs no responsibility nor any obligation whatsoever; and the fact that the Government may have formulated, furnished, or in any way supplied the said drawings, specifications, or other data, is not to be regarded by implication or otherwise as in any manner licensing the holder or any other person or corporation, or conveying any rights or permission to manufacture, use, or sell any patented invention that may in any way be related thereto.

Copies of this report should not be returned to the Research and Technology Division unless return is required by security considerations, contractual obligations, or notice on a specific document.

200 - March 1967 - CO192 - 27-613

MICROPHONE SYSTEM FOR THE MEASUREMENT OF BOUNDARY LAYER PRESSURE FLUCTUATIONS

J. C. ORTEGA

WESTERN ELECTRIC-ACOUSTIC LABORATORY, INC.
LOS ANGELES, CALIFORNIA

FOREWORD

The research in this report was performed by Western Electro-Acoustic Laboratory, Los Angeles, California, for the Flight Dynamics Laboratory, Research and Technology Division, Air Force Systems Command, Wright-Patterson Air Force Base, Ohio, under Air Force Contract No. AF33(615)-2544. The Air Force program monitor was Mrs. P. G. Bolds, FDDS. The research was conducted from May 1965 to July 1966, and the report was submitted in August 1966.

The author of this report is Jose C. Ortega of Western Electro-Acoustic Laboratory. The author wishes to express his appreciation to Mr. Paul S. Veneklasen, Director of Western Electro-Acoustic Laboratory, for guidance during the program work, to Mr. John W. Little, formerly of WEAL, for his contributions in the early phases of the program, and to the staff of WEAL for their overall support. In addition, the author acknowledges the capable assistance of Mr. Robert Bridwell of Norair Division, Northrop Corporation, in the performance of the microphone temperature response measurements.

This technical report has been reviewed and is approved.

WALTER J. MYKYTOW
Asst. for Research & Technology
Vehicle Dynamics Division

ABSTRACT

This report presents a description of a condenser microphone system developed for use in the measurement of boundary layer pressure fluctuations. Prime consideration in the design of the transducer of the system was the requirement for operation in abnormal environments, with emphasis on high temperature. Calibrations are described in the report which show that the Western Electro-Acoustic Laboratory A-6 condenser microphone can operate at diaphragm temperatures to 800°F.

Measurements utilizing an electrical analog of the microphone thermal characteristics and flat plate boundary layer theory show that an 800°F upper limit for the transducer would satisfy nearly all conceivable uses of the system in practice. For example, for a "flight" condition of Mach 4.2 at sea level, where the recovery temperature would be 1600°F, the diaphragm temperature would reach 800°F. This same speed at 40,000 ft. would result in a diaphragm temperature of 300°F. A speed of Mach 6.9 would be required to produce an 800°F diaphragm temperature at 40,000 ft. These flight conditions are extreme for present day vehicles, including re-entry vehicles, hence the transducer can be used over a very large range of altitudes and Mach numbers.

This report presents the methods and results of calibration, as well as some of the shortcomings of the system.

TABLE OF CONTENTS

Table of Contents (continued)

LIST OF ILLUSTRATIONS

List of Illustrations (continued)

LIST OF SYMBOLS

a	acceleration
a_D	condenser microphone active diaphragm radius
a_B	condenser microphone backplate radius
c	wave velocity in condenser microphone diaphragm
c_A	velocity of sound in air or other medium
c_f	skin friction coefficient for compressible flow
c_{fi}	skin friction coefficient for incompressible flow
c_p	specific heat of air at constant pressure
db	decibel
e	microphone output voltage
f	frequency
g	acceleration due to gravity
k	a constant for a parallel plate capacitor depending on the unit used for the dielectric constant
p	acoustic pressure
p_o	reference acoustic pressure
q	charge produced by a capacitive transducer
s	distance between condenser microphone diaphragm and backplate
t	time
t	condenser microphone diaphragm thickness
r	space coordinate

List of Symbols (continued)

z	condenser microphone diaphragm specific acoustic impedance
A	Amplitude of the average diaphragm displacement of a condenser microphone
B	A condenser microphone parameter
C	Condenser microphone electrical capacitance
$C_f = \frac{c_f}{c_{fi}}$	Ratio of the skin friction coefficient
E	Charge amplifier output voltage; voltage across a condenser microphone
E_o	Condenser microphone polarizing voltage
E_T	Amplifier threshold noise
G	Charge amplifier gain
$\dot{H}$	Heat flow rate
$H(\gamma, \mu)$	Condenser microphone frequency response parameter
$J(\gamma, \mu)$	A Bessel function parameter
J_o	Bessel function of the first kind of zero order
J_1	Bessel function of the first kind of first order
J_2	Bessel function of the first kind of second order
$K = \frac{\rho c_A^2 \pi a_e^4}{\gamma V}$	Condenser microphone cavity stiffness parameter
KCPS	Kilocycles per second
M	Condenser microphone acoustic sensitivity
M_{oc}	Low frequency condenser microphone acoustic sensitivity
$N = c_p \rho_e U_e \times 10^{-3}$	A boundary layer parameter
P_o	Atmospheric pressure

List of Symbols (continued)

P_E	Static pressure acting on diaphragm of a condenser microphone due to a polarizing voltage
P_M	Static pressure acting on diaphragm of a condenser microphone due to an altitude change
Q	Electric charge on a condenser microphone
Q_{oc}	Open circuit charge sensitivity of a condenser microphone
R	Real part of the specific acoustic impedance z acting on the diaphragm of a condenser microphone
SPL	Sound pressure level in db re .0002 dyne/cm^2
R_{BW}	Heat flow resistance between condenser microphone backplate and wall
R_{WS}	Heat flow resistance between microphone wall and heat sink
S	Condenser microphone backplate area
T	Condenser microphone diaphragm temperature
T_o	Ambient air temperature
T_B	Microphone backplate temperature
T_W	Microphone wall temperature
T_R	Recovery temperature
T_S	Heat sink temperature
U_e	Velocity of air at outer edges of the boundary layer
V	Condenser microphone cavity volume
X	Imaginary part of the specific acoustic impedance z
Z_A	Acoustic impedance of the microphone cavity

List of Symbols (continued)

$\beta = \frac{\omega r}{c}$	Bessel Function frequency parameter
$\gamma = \frac{\omega a_B}{c}$	Bessel Function frequency parameter
$\mathcal{J}$	Microphone diaphragm specific acoustic impedance ratio
η	Microphone diaphragm displacement
$\bar{\eta}$	Average microphone diaphragm displacement
Θ	Real part of the microphone diaphragm specific acoustic impedance ratio
K	Thermal conductivity
$\mu = \frac{\omega a_p}{c}$	Bessel function frequency parameter
ρ	Density of microphone cavity medium
ρ_e	Density of air at outer edge of boundary layer
ρ_s	Surface density of microphone diaphragm material
σ	Condenser microphone diaphragm stress
τ	Condenser microphone diaphragm tension
ϕ	Space coordinate
χ	Imaginary part of the microphone diaphragm specific acoustic impedance ratio
$\omega = 2\pi f$	Angular frequency
∇	Laplacian operator
$\Delta(\gamma, \mu)$	A Bessel function parameter

SECTION I

INTRODUCTION

Scientific interest in the measurement of boundary layer pressure fluctuation dates back to early studies by aerodynamicists in the effort to understand the phenomenon of the boundary layer which is associated with high speed gas flow near a moving surface. Later, the problem of boundary layer noise, or "psuedo noise" as it is often referred to, stimulated interest in the commercial transport field in the effort to reduce cabin noise in flight. More recently, the need to measure accurately the fluctuating pressures in the boundary layer has been increased by the development of very high speed aircraft and orbiting re-entry vehicles. Here the need for measurement transducers with high temperature operating capability is an important requirement. The measurement is of increasing importance as increased speeds, surface temperatures, and boundary layer psuedo noise magnify the problems of interior noise control, fatigue tolerance of materials and component failures.

In 1963 this laboratory developed, under contract with the Air Force (AF33-616-4331) a microphone (WEAL Type A-3) and preamplifier (WEAL Type 151-A) for use in the measurement of boundary layer pressure fluctuations which have high temperature capability (Ref. 1). Calibration of this condenser microphone system showed that repeated operation, with diaphragm temperatures as high as 600°F, could be achieved with no damage to the system. The system has proven successful in measurement of the pressure fluctuations in the turbulent boundary of a re-entry vehicle (Ref. 2) with its attendant high temperatures and dynamic pressures.

Even with the stated success of the A-3 microphone system, it was apparent that certain potential improvements to the system should be further investigated. The contract work which led to the development of the A-6 microphone and associated electronics is a continuting effort for improvement of the earlier system. This report has as its purpose the presentation of a description of the improved system, along with details of the studies which led to the final design. In addition, the results of testing and calibrations of the microphone system are presented.

The work in this program had several objectives relative to the improvement of the A-3 condenser microphone system. These program objectives included the following:

(a) The investigation of an improved microphone design utilizing a guard ring to create a physical and electrical shield between microphone backplate and ground potential. The guard ring would serve to reduce stray capacity signal losses between microphone and preamplifier. This guard ring would also improve the heat flow path between microphone diaphragm and microphone interior assembly, thereby reducing diaphragm temperatures and also improving diaphragm temperature uniformity.

(b) The study of sealant insulating materials which could withstand high temperatures and not be permeable to helium, but retain all of the characteristics required by the microphone system.

(c) Studies to determine the feasibility of utilizing "charge" or current amplifiers in conjunction with condenser microphones to replace the cathode follower normally used.

(d) Studies to determine the feasibility of reducing the size of the microphone by decreasing the diameter of the microphone outer shell.

(e) Investigation of the use of thinner diaphragm stock to increase the acoustic sensitivity and decrease the mechanical vibration sensitivity of the microphone.

(f) Incorporation of a guard ring in the microphone presupposes a preamplifier design which would allow separation of microphone and preamplifier so that the preamplifier could be designed for far less severe environments than for the microphone. Hence, an extensive design study of the preamplifier was considered necessary.

(g) Past experience has shown that design of a high temperature microphone is greatly facilitated by the use of an electrical analog of the microphone which allows quantitative temperature data to be obtained for various flight parameters. It was decided that after preliminary design of the microphone and associated connectors, an analog would be designed, fabricated and used. The results would define completely the thermal conditions in the microphone, including the radial temperature contour on the diaphragm for the design configuration of the microphone and for a very large range of vehicle flight parameters.

(h) Past methods used for determination of the effects of altitude and temperature in microphone operation have been unsatisfactory from the point of accurate environmental simulation. In particular, it is felt that the microphone response to a combined altitude-temperature environment has not been adequately defined. Part of the work in this program, therefore, was allotted for improvement in experimental techniques for this type of calibration.

The remainder of the report is divided into sections which present the results of studies carried out during the program. Section II presents findings relative to the use of a charge amplifier in conjunction with a condenser microphone. Section III is a description of the microphone, microphone connector and high temperature co-coaxial cable. Section IV describes the electronic package, while Section V presents the results and conclusions of the heat transfer analog studies. Section VI deals with system calibration, test methods and results. Section VII presents conclusions and recommendations for future research. Finally, the appendix includes theoretical studies

which were used as a guide in formulation of final microphone design.

We note that the proposed use of the system as an experimental laboratory piece of equipment has led to concentration in the improvement of overall system performance for this type of application. For this reason, miniaturization of the system, particularly the electronics, was not considered of paramount importance. However, the concepts incorporated in the improved electronic design have in fact been specifically conceived with the prospect of miniaturization for use in airborne applications.

With respect to the system performance, it is noted here the final design is a significant improvement over the previous microphone system. Many of the design objectives are met or exceeded. Some of the target specifications are clarified; others must be modified. Some of the performance characteristics which fall short of the target specifications are the result of compromises made in order that another performance characteristic of more importance be achieved for total optimization.

SECTION II

CHARGE AMPLIFIER STUDY

The use of charge amplifiers in conjunction with capacitive transducers, such as piezoelectric microphones and accelerometers, has recently become widespread. The condenser microphone being a capacitive transducer, can also be used in conjunction with a charge amplifier if a stable polarizing voltage is supplied to the microphone. It was decided, therefore, to investigate the use of a charge amplifier in conjunction with a condenser microphone and the results of this study are presented in this section.

Our investigation shows that a charge amplifier system would have serious limitations which preclude its use in this program. In brief, these limitations stem from the inherent high threshold noise levels exhibited by available charge amplifiers. Our investigation of commercially available units shows that typical threshold noise levels range from 1 mv to 5 mv with fully transistorized airborne units exhibiting lower levels, and laboratory type units higher levels. This limitation reflects in a higher value of the minimum sound pressure levels which can be measured and in a smaller dynamic range of sound pressure. These points are discussed further in the paragraphs to follow:

A. Threshold Noise

Our investigation into the use of charge amplifiers in conjunction with a condenser microphone necessitated a study of threshold noise levels. A charge amplifier was loaned to WEAL by Endevco Corp. (Type 2620) for use in this investigation, and measurements of a system employing this amplifier were performed. The results of our measurements in octave bands are presented in Table I below.

Table I

Measured Noise Thresholds on an Endevco Charge Amplifier Type 2620

	Octave bands, cycles per second								
	Over -all	0 75	75 150	150 300	300 600	600 1200	1200 2400	2400 4800	Above 4800
Threshold noise (mv)	.6	.4	.1	.02	.02	.02	.02	.02	.1

As shown in the table, the overall level was .6 mv, which is slightly lower than the manufacturer's stated threshold noise level for this unit. Hence, we apparently were dealing here with a "quiet" unit. We also point out here that these measurements were performed at a low gain setting of the amplifier. This particular unit has higher threshold

noise levels at high gain settings. Hence, the above measured values are the lowest obtainable from the unit.

In order to evaluate these data it is necessary to convert these voltage values to equivalent sound pressure levels in terms of the charge sensitivity of the proposed condenser microphone. The acoustic open circuit charge sensitivity of a condenser microphone is related to its acoustic open circuit voltage sensitivity by the relation

$$Q_{oc} = M_{oc}C \tag{1}$$

where Q_{oc} = open circuit charge sensitivity (coul/dyne/cm^2)

M_{oc} = open circuit voltage sensitivity in volts/dyne/cm^2

C = microphone capacity in farads

Equation (1) makes it quite clear why piezoelectric transducers can be used with charge amplifiers without a threshold noise problem. A condenser and piezoelectric microphone of equal voltage sensitivity can have vastly different charge sensitivity if their capacitance differs greatly. Typical values of capacitances for piezoelectric microphones (which cannot meet the thermal requirements of this program) are on the order of 100 times greater than for condenser microphones. This amounts to a charge sensitivity difference of 40 db if their voltage sensitivities are equal.

From (1) above it is clear that the charge (q) produced by a condenser microphone, when subjected to a sound pressure p, is

$$q = Q_{oc}p \quad \text{(coul)} \tag{2}$$

$$= M_{oc}Cp \quad \text{(coul)}$$

and also that the output voltage of a charge amplifier (E) used in conjunction with a condenser microphone is

$$E = M_{oc}C\,p\,G \text{ (millivolts)} \tag{3}$$

where G is the gain of the charge amplifier in (millivolts/coul).

If we allow a minimum signal-to-noise ratio of 15 db, then we have the condition

$$\frac{E}{E_T} \geq 5.62$$

where E_T is the threshold noise voltage.

Therefore, we have

$$p \geq \frac{5.62\, E_T}{M_{oc}\, C\, G}$$

where p is the sound pressure in dynes/cm^2 required to achieve a minimum 15 db signal-to-noise ratio.

Taking the following parameters for the A-6 microphone and the gain used, and threshold measured with the model 2620 charge amplifier, we can arrive at the minimum sound pressure levels which can be measured with this system.

E_T = threshold noise (mv) (see Table I)

$G = 2.4$ mv/pico coul

$= 2.4 \times 10^{12}$ mv/coul

$C = 10 \times 10^{-12}$ farads

$M_{oc} = 5 \times 10^{-5}$

$= -86$ db re 1 volt/dyne/cm^2

The values of the minimum sound pressure levels are given in Table II below

Table II

Minimum Sound Pressure Levels Measurable with Charge Amplifier System

	Octave bands, (cycles per second)								
	Over -all	0 75	75 150	150 300	300 600	600 1200	1200 2400	2400 4800	Above 4800
E_T (mv)	.6	.4	.1	.02	.02	.02	.02	.02	.1
Minimum sound pressure level (db re. 0002 dyne/cm^2)	143	139	127	113	113	113	113	113	127

It is clear that the charge amplifier threshold noise imposes an unacceptable lower

sound pressure level limitation on the system.

B. Dynamic Range

The charge amplifier system dynamic range is actually limited by the lowest measurable sound pressure level. Typical maximum output levels are 1.77 volts rms. Assuming a microphone voltage sensitivity of 5×10^{-5} volts/dyne/cm^2 and a capacitance of 10 picofd, this output corresponds to an upper sound pressure level of 197 db. Hence, the dynamic range would be from 143 to 197 db, or 55 db. Since levels on the order of 197 db are beyond our limits of interest, it is obvious that the dynamic range of a charge amplifier system is neither wide enough nor centered appropriately on the sound pressure level scale.

The need of a very stable polarizing voltage across the terminals of a condenser microphone imposes a further requirement on a charge amplifier if it is to be used in conjunction with a condenser microphone. At present, charge amplifiers are not manufactured with this feature and even if the limitations discussed above could be overcome, further electronic design would be required.

The principal advantage that a charge amplifier exhibits is the ability to separate transducers from amplifiers without serious signal losses in the separating cable. However, this same advantage can be obtained with a specially designed preamplifier circuit with lower inherent noise. For this reason it was concluded that a voltage preamplifier is preferable to a charge amplifier and the remainder of the report is based on use of a preamplifier which is described fully in Section IV.

LEGEND

1. Diaphragm
2. Microphone outer shell
3. Expander ring
4. Inner shell
5. Locking ring
6. Microphone guard ring
7. Backplate
8. Glass tube
9. Locking washer
10. Connector center pin
11. Connector guard ring
12. Connector outer shell
13. Connector assembly ring
14. Connector base
15. Insulator, Pyroceram No. 95
16. Co-coaxial cable
17. Silicone rubber

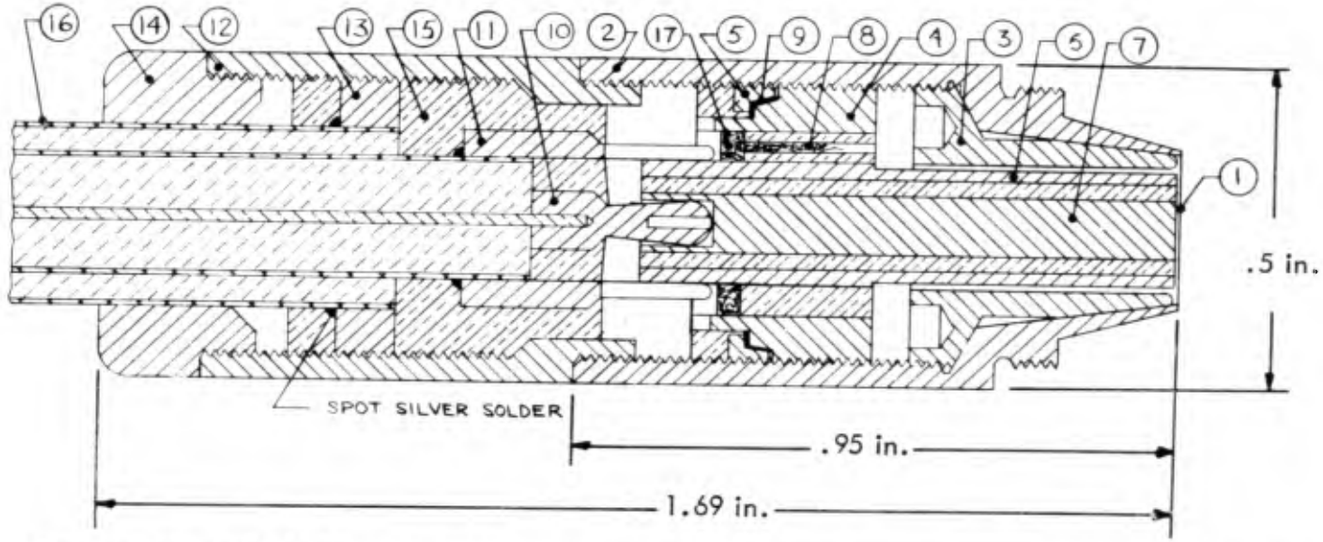

Figure 1. Cross section of WEAL Type A-6 condenser microphone, microphone connector and co-coaxial cable.

SECTION III

MICROPHONE, CONNECTOR AND CABLE DESIGN

A. Microphone Size Reduction

Figure 1 presents design details for the complete A-6 microphone and connector assembly. Also shown is the junction between connector and co-coaxial cable. The results of this part of the study program demonstrated the feasibility of significant size reduction for both microphone and connector. The diameter of the microphone's diaphragm has not been changed from the design of the earlier WEAL A-3 microphone (.250 in.). Likewise, the dimensions of the expansion cone have been retained. In all other dimensions the A-6 microphone is smaller than the A-3. The A-6 microphone has a maximum diameter of 0.50 inch and an overall length of .95 inch. The connector shell is also 0.50 inch in diameter. The combination has an overall length of 1.69 inches. For comparison, the A-3 microphone has a diameter of 0.985 inch and a length of 1.20 inches. The combined length of A-3 microphone and 151A preamplifier is 3.485 inches.

We do not feel that the reductions were achieved at the expense of structural integrity. Wall thicknesses are less than on the A-3 but smaller circumferences increase rigidity. Furthermore, the size reductions attained were, in large part, made possible by the use of the sealing material as a foundation for assembly. Hence, bulky locking rings are eliminated. In our opinion, the "potted" assembly is structurally more rugged and durable.

The reduced size offers other advantages because of reduced weight and space requirements. Also, the smaller shell diameter permits closer proximity between adjacent microphones, which is an advantage in boundary layer correlation work.

B. Guard Ring Design

Reference to figure 1 again will show the development of the guard ring concept in the microphone, connector and cable. It is seen that the guard ring physically creates an electrical shield between the backplate of the microphone and the ground potential of the shell. The use of this concept provides several improvements in microphone design, which are listed here.

(1) The guard ring reduces the effective stray capacitance between the microphone and the grid of the first stage of the preamplifier (see figure 6). The effect of this reduction of stray capacitance is an effective increase in output signal from the microphone, since stray capacitance is electrically in shunt with the active capacitance

of the microphone, reducing microphone signal to the grid of the cathode follower in the preamplifier.

(2) The potential electrical leakage between the microphone backplate and the shell is reduced by the guard ring connection to the cathode follower circuit.

(3) The presence of the guard ring improves the heat flow path from the diaphragm to the backplate assembly. The design of the guard ring results in a more uniform diaphragm temperature profile at all elevated temperatures, thus making the prediction of microphone characteristics more reliable. (See Section V.)

(4) The use of the guard ring makes it possible to locate the microphone at some distance from the cathode follower preamplifier, thereby eliminating the need of a cathode follower with very high temperature capabilities.

It can be seen on figure 1 that the guard ring is positioned as close to the diaphragm as is physically possible to provide maximum electrical shielding between backplate and ground. This design also insures maximum heat transfer from the diaphragm to microphone interior.

C. Materials

(1) Microphone and connector machined parts

All machined metal parts of the microphone and connector, except one, are made of PH 15-7 Mo stainless steel heat treated to the RH 950 condition to provide maximum strength. Figure 2 shows the 0.2% yield and tensile strength of this material as a function of temperature.

The selection of this material over many others considered was based on an evaluation of many properties of the material, including (a) high temperature yield strength, (b) high temperature corrosion resistance, (c) coefficient of thermal expansion, (d) thermal conductivity, and (e) machinability.

There is one metal part in the microphone which is not made from PH 15-7 stainless steel. This is the 3-lobed brass locking washer between the locking ring and inner shell to aid in the positioning and locking operation during which the backplate-diaphragm spacing is set. (See figure 1).

(2) Microphone diaphragm material

The diaphragm is also PH 15-7 Mo stainless steel, since our studies show this material is superior in overall qualities to other possible materials.

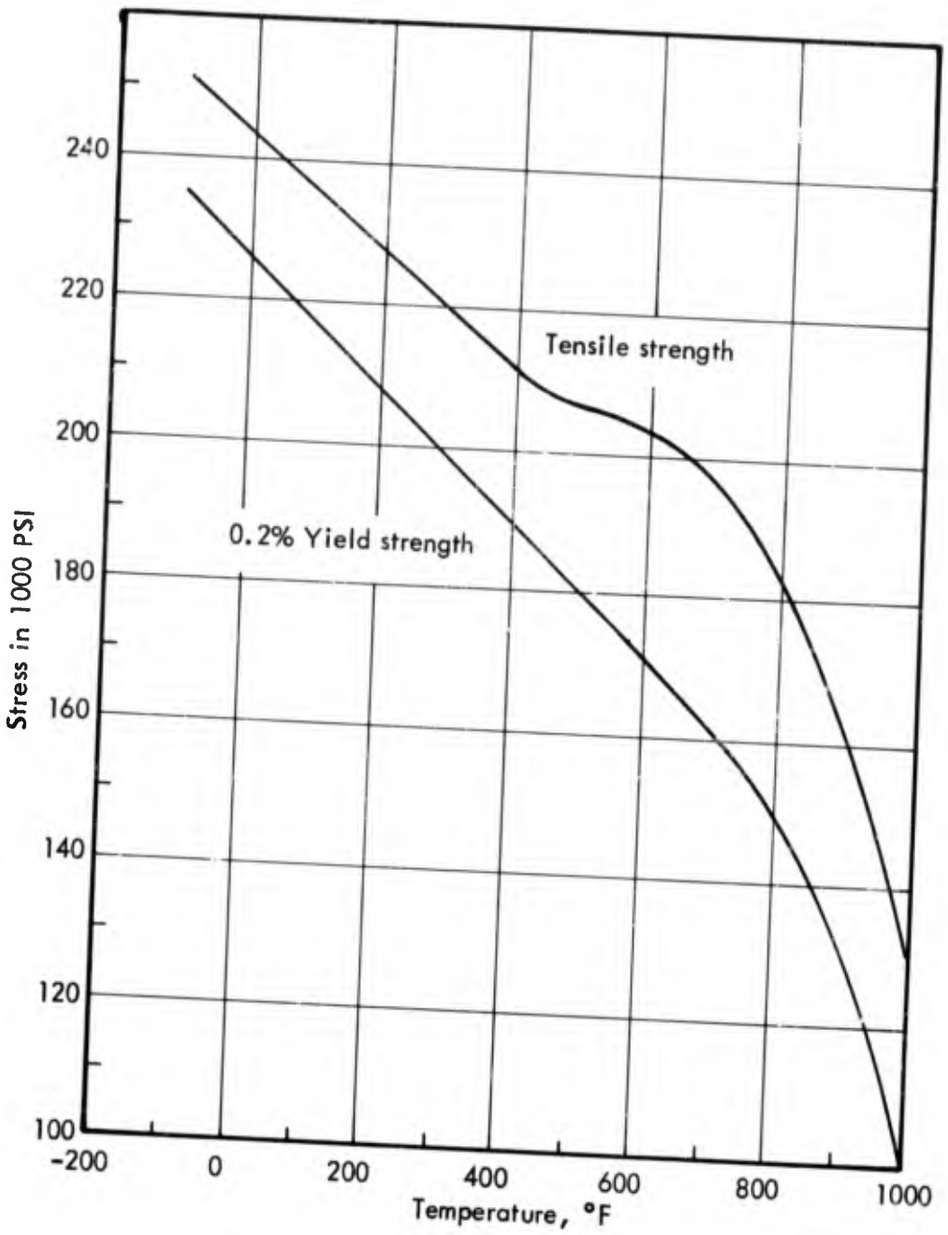

Figure 2. Tensile and .2% yield strengths of PH 15-7 M_o stainless steel in a RH 950 heat treat condition versus temperature

The diaphragm thickness used in the A-3 microphone was .00075 inch and it was contemplated that a thinner diaphragm stock for the A-6 microphone would be advantageous in that an increase in acoustic sensitivity, and at the same time a reduction in vibration sensitivity of the microphone could be achieved. However, our studies showed that reducing diaphragm thickness is in conflict with the desire to limit variations in microphone response due to change in altitude. (see Appendix) This conflict comes about because of the stress limitations of the material itself. Stress-strain data shown on figure 2 for PH 15-7 Mo stainless steel indicate a .2% yield strength of 150,000 lbs/in. at 800°F. Since this is the heat soak design limit, it was decided to limit diaphragm stress accordingly. Now, since stress (σ) and tension (τ) are related via the diaphragm thickness (t) by the relation $\tau = \sigma t$, it is clear that once σ is chosen, τ is a function of t, or vice versa, t is a function of τ. Our studies of the effect of pressure differential or altitude on the microphone sensitivity show that in order to minimize changes with altitude, a maximum value of τ is desirable. This means that for a given maximum stress, the diaphragm thickness must be maximized.

Calculations were performed using final microphone dimensions for four different diaphragm thicknesses to show the change in microphone sensitivity when subjected to one atmosphere of pressure differential (infinite altitude) and the results are presented in Table III below. The diaphragm stress for each of the three thicknesses was 150,000 lbs/in^2. Note that the $.6 \times 10^{-3}$ in. diaphragm thickness would very nearly satisfy the target specification of -3 db.

Table III

Calculated A-6 Microphone Sensitivity Loss Versus Diaphragm Thickness

Diaphragm thickness (in.)	Diaphragm tension (dyne/cm)	Loss at 1 atmosphere pressure differential (db)
.0006	1.58×10^7	4.0
.0005	1.314×10^7	4.6
.0003	7.89×10^6	6.7
.0001	2.63×10^6	13.1

Our earlier investigation of available diaphragm materials has shown that minute holes are likely to be present when material thicknesses are less than about .0005 inch. The presence of these pinholes, which incidentally are not visually apparent to the naked eye, probably indicates a non-uniform diaphragm thickness which is not desirable. In addition, our desire to retain helium in the microphone precludes diaphragm

material which potentially has holes in it. Based on the above considerations, it was decided to use the .0006 inch thick material in the construction of the A-6 microphone.

(3) Sealing material

The study of sealing materials focused attention on three areas: (a) high temperature endurance, (b) helium impermeability and (c) general compatibility with the other system requirements.

The survey of candidate materials looked first for high temperature endurance. A target specification of 600°F soak conditions was established. Next, information was needed on the helium permeability of those materials which were being studied. Unfortunately, this information is not normally supplied and we were forced to prepare samples which we could test. Previous experience and study showed that helium impermeability is not a typical characteristic of the type of materials we were studying. It began to appear that we would have to find a material that would not pass helium, and then design the microphone around it. We subsequently prepared samples of several materials that could conceivably be used and performed helium leak tests utilizing a mass Spectrometer Helium Leak Detector. The results of this study are summarized in Table IV. The reciprocal leak rates shown indicate the amount of time it would take for practically all the helium to leak out of a sealed microphone. Also shown are manufacturer's suggested long time service temperatures.

At the start of the permeability studies we arbitrarily set a minimum reciprocal leak rate of 2 yrs/cc^2. As seen on Table IV, permeability rates tend to be very short or very long. Obviously, the materials with reciprocal leak rates on the order of days are unacceptable. Many materials that reportedly were capable of high temperature performance were discarded because they were so similar to the ones which failed the helium test.

The selection was now narrowed to the three materials at the bottom of Table IV, and consideration was given to the other properties of the materials and those compared with the overall requirements of the system. The Pyroceram cement was selected for several reasons. First, all curing and handling processes could be performed by our own personnel, using our laboratory equipment. Second, the curing process and characteristics of the material were somewhat compatible with the procedures used in the microphone assembly and adjustment. Third, all the physical properties of the pyroceram cement matched those of the steel components of the microphone. Tests have shown complete compatibility of the two materials.

The other two materials which met the temperature and helium retention specifications were discarded primarily because the molding and curing processes could be performed only by the manufacturer. We were also led to understand that the micalex

Table IV

Summary of Helium Leak Rates for Several Sealing Materials

Material	Manufacturer	Designation	Preparation	Reciprocal of Leak Rate	Service Temperature
Silicone rubber	General Electric	RTV-60	Air cured	1.35 days/cm^3	600°F
"	" "	"	Vacuum cured	"	600°F
"	" "	LTV-602	Air cured	3.0 days/cm^3	300°F
"	" "	"	Vacuum cured	2.09 days/cm^3	300°F
"	Emerson & Cumming	Eccosil 4640	Air cured	4.82 days/cm^3	600°F
Silicone varnish	General Electric	SR-155	Oven cured	8.43 days/cm^3	480°F
Alumina ceramic	Coors	96% alumina	Furnace fired[1]	Impermeable[2]	2800°F
Ceramoplastic	Mycalex Electronics	Supramica 620 "BB"	" " [1]	"	1200°F
Pyroceram cement	Owens-Corning	Brand #95	" " [3]	"	825°F

Notes: 1. This material can be prepared only within the manufacturer's facilities.

2. The word "impermeable" is used in this table to indicate that the test equipment could detect no leakage of helium during a reasonable long test period. The minimum leak detecting capability of the mass spectometer used was 1.32×10^{-9} cm^3/sec or in terms of the above, this is equivalent to 24 years/cm^3.

3. All curing of this material can be performed in our laboratory.

4. All samples tested in this table were tested utilizing an effective cross-sectional area for helium flows of 1.96×10^{-1} in^2, and a thickness of approximately .125 in.

material could not be successfully used in the thin spaces of the microphone inner assembly. Furthermore, there did not appear to be any way to seal the fully assembled microphone with helium because the curing temperatures for these materials exceed the upper limit of the stretched diaphragm. In this respect, the Pyroceram curing temperature of 825°F appeared to be a good match with the design parameters of the microphone.

Subsequent work using the Pyroceram in the attempt to seal the microphone showed that the 825°F curing temperature did affect the tension on the microphone diaphragm. A microphone with an initial diaphragm resonant frequency of 44 KCPS when subjected to a one-half hour cure of 825°F had this value reduced to 38 KCPS. This amounted to about a 2.5 db increase in acoustic sensitivity and also to a greater response to altitude changes. The latter factor is undesirable. Further experimentation with curing times and temperatures showed that longer cures and lower temperatures could be used to obtain satisfactory cures of the Pyroceram. This method reduced changes in microphone resonant frequencies and sensitivity to tolerable values (41 KCPS for resonant frequency and a 1 db change in sensitivity) and was used in the subsequent assembly and sealing of the microphones.

4. Glass tube

The glass tube molded into the Pyroceram glass (see figure 1) is used to simplify the helium seal process. After the backplate is positioned and locked, an additional layer of Pyroceram will be used to seal the entire assembly, leaving only the small glass tube as entrance to the microphone cavity. It was originally planned to seal the helium in the microphone by sealing the end of the glass tube, using a small butane torch while the microphone was in a pure helium atmosphere. Practically, this proved to be extremely difficult. Several attempts using the procedure resulted in failure, with the helium in the cavity leaking out in an hour or two. It was also determined that the leak was located at the tube end, indicating a faulty seal at that point. Examination of the fused tube end indicated glass flow but with minute bubbles. It can only be surmised that minute cracks were also present, these being the result of stresses set up in the glass while cooling. At this juncture the method of sealing was reviewed and it was decided to investigate the use of the silicone rubber as a means of sealing the small bore glass tube already molded into the backplate assemblies. Using the data of Table IV, the permeation constant for the RTV-60 silicone rubber was calculated and found to be about 2.83×10^{-7} (cm^3-mm/sec. - cm^2-cm-Hg). This value, while much larger than the permeation constant for the Pyroceram, was still small enough to warrant further investigation. Using this value and the physical dimensions of the small bore glass tube, it was calculated that the leak rate through the tube filled with RTV-60 silicone rubber would be 7×10^{-8} sec/cm^3, or 22.2 yrs/cm^3. In other words, with very small cross-sectional areas for helium flow, the silicone rubber can be used. It was then decided to take this approach in the helium sealing of the microphone. To further ensure that a small cross-sectional area for the helium flow be encountered by the permeating helium, the end of the glass tube was plugged, using a small solid glass plug. Measurements made

on the sealed microphones as long as 10 weeks after sealing indicate that no measurable helium permeation has occurred.

5. Helium

The microphone is assembled in a pure helium atmosphere and sealed as discussed above. The purpose of the helium-filled sealed cavity is four-fold. First, a sealed cavity ensures that the acoustical properties of the microphone are essentially independent of altitude. It is known that an unsealed condenser microphone at high altitude has an output at its resonant frequency which is on the order of 60 decibels higher than its output below resonance. This occurs because the damping which is provided by the thin film of gas between the diaphragm and backplate at normal pressure is eliminated, or greatly reduced at high altitudes. This phenomenon can render measured data meaningless. Second, the helium gas in the cavity minimizes the heat flow resistance (increases rate of heat flow) between the microphone diaphragm and backplate, thus reducing diaphragm temperature. (see Section V) Helium gas has a thermal conductivity about eight times that of air. Third, the assembly of the microphone in a dry helium atmosphere aids in keeping all microphone parts free of dirt or dust and also ensures that no moisture is trapped in the microphone cavity. Fourth, because the microphone is completely sealed, it is not subject to moisture contamination of the interior assembly.

D. Diaphragm Brazing

Previously used brazing techniques and material have been changed to provide improvement in two areas. First, the achievement of a perfectly flat diaphragm depends to some extent on the size of brazing alloy fillet formed in the microphone interior. If this fillet is too large, stretching of the diaphragm tends to form a concave crease on the diaphragm along the line formed by the inside periphery of the brazing alloy. In order to minimize this fillet, we have designed the diaphragm-shell joint as shown on figure 3. This design is intended to carefully control placement and quantity of brazing alloy.

Second, our past experience showed that stretched diaphragms subjected to soak temperatures of 825°F would lose tension and suffer a permanent decrease in resonant frequency. The microphones on which this was observed were assembled so that the temperature limit of the steel was on the order of 950°F. Hence, it was concluded then that the weakness must exist in the high temperature tensile strength of the brazing alloy. Based on these conclusions, a eutectic alloy (produced by Handy & Harmon Co.) was selected, which melts and flows at 1740°F. (Primabraze 130, 82% Au, 18% Ni). This melting and flow temperature is compatible with the 1750°F temperature required for the austenite conditioning phase of the heat treat cycle. It was believed that this alloy selection would eliminate the changes in diaphragm tension noted above. This has not proved to be the case, as noted earlier in this section. However, the new alloy is still considered to be an improvement over the earlier one used.

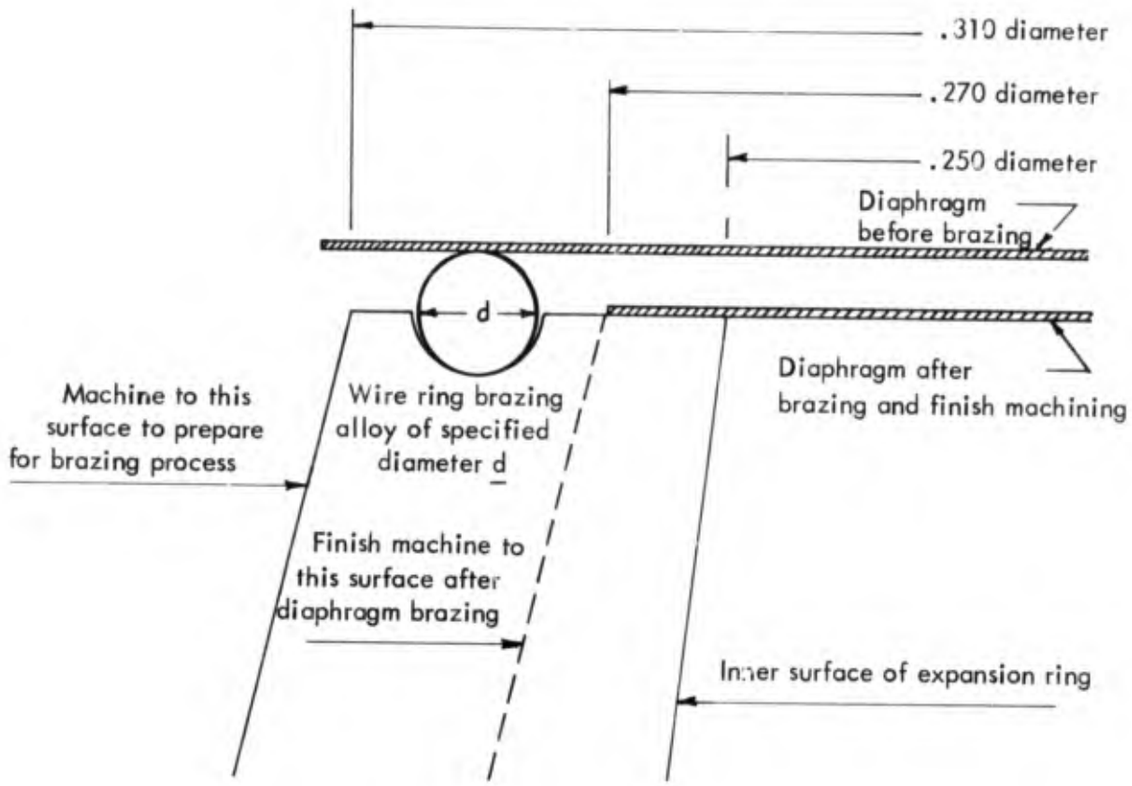

Figure 3. Section view of brazing and machining details at joint between microphone diaphragm and expansion cone.

E. Co-coaxial Cable

The design details for the selected co-coaxial cable are shown on figure 4. The dimensions of the cable components determine the cable capacitances which were used in the design of the electronic system. Our investigation into the available co-coaxial cables which could be used between the microphone and preamplifier revealed none which possessed the required temperature capability. It was required, therefore, to have a small quantity of a specially designed cable manufactured for use in this program.

The measured capacitance of the cable, which is a function of cable dimension, showed it to be compatible with the electronic design and in this respect was appropriately

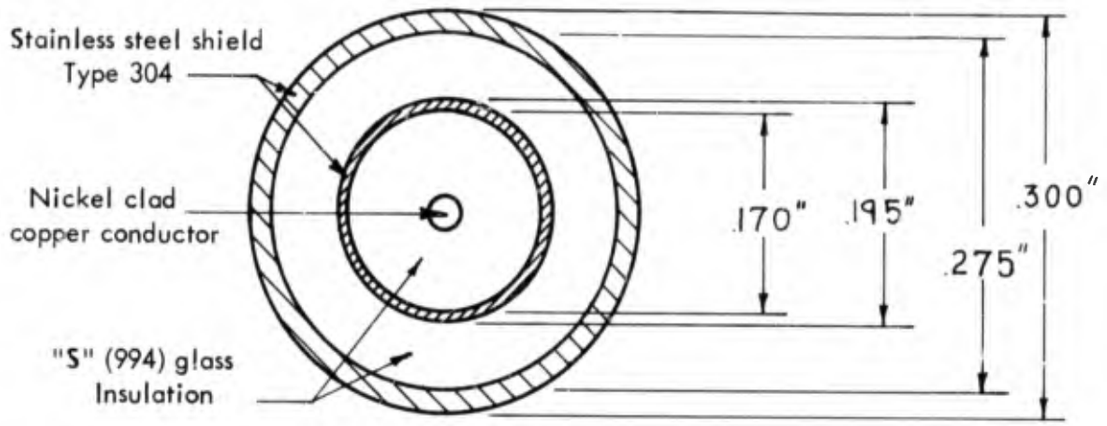

Figure 4. Schematic diagram of high temperature co-coaxial cable for use with high temperature microphone.

designed. The use of the spun glass insulation in the cable solves the high temperature problem; however, it does result in a cable that tends to be somewhat microphonic. The compliance of spun glass insulation allows relative movement between signal conductor and inner and outer shields when subjected to vibration. The results of the vibration tests are discussed further in Section VI.

SECTION IV

ELECTRONIC DESIGN

This section describes the design of microphone system preamplifier and amplifier and also presents the performance characteristics. Discussion is facilitated by reference to figure 5, which shows in block diagram form the microphone system. The separation of microphone from preamplifier by 20 ft. of cable allows the preamplifier to be designed without extreme environmental capabilities which would add considerably to the system cost. It is felt that this scheme makes for a more reliable system, since it reduces to a minimum the number of components exposed to extreme environments and therefore reduces chances for failure. A separation of 20 ft. should be sufficient for most conceivable uses.

The design of the preamplifier allows a separation between it and the power supply and amplifier of up to 250 ft. without affecting system characteristics in any way. With this capability and the fact that all important system functions are monitored at the power supply, the convenience of control room rack or console mounting is achieved.

A. Preamplifier

The circuit diagram of the preamplifier is shown in figure 6. This circuit, which is an advanced version of an earlier design (Ref. 3), feeds a signal from the first stage cathode follower through an additional amplifier, and then feeds back this signal in proper phase to the cathode of the first stage cathode follower. The chief advantage of this circuit is that the effective input impedance of the first stage cathode follower is greatly magnified with the result that a relatively long cable between microphone and preamplifier can be used.

The frequency response and insertion loss through the preamplifier can be controlled by the proper amount of signal feedback to the cathode of the first stage. This means that the amount of feedback is controlled by the values of C5, C6, C8 and R12. We note that the values chosen for the design are based on 20 ft. of co-coaxial cable of the type shown in figure 4. Use of a different length of cable would necessitate a change in these circuit parameters to achieve flat frequency response and unity gain of the preamplifier.

The frequency response of the Type F preamplifier is shown in figure 7. The response is seen to be flat within ±1 db from 25 CPS to 50 KCPS. We note here that flat frequency response to 10 CPS was obtainable at the expense of a greater signal insertion loss and was not deemed desirable since increase in insertion loss meant less signal-to-noise ratios for measurement of low sound pressure levels.

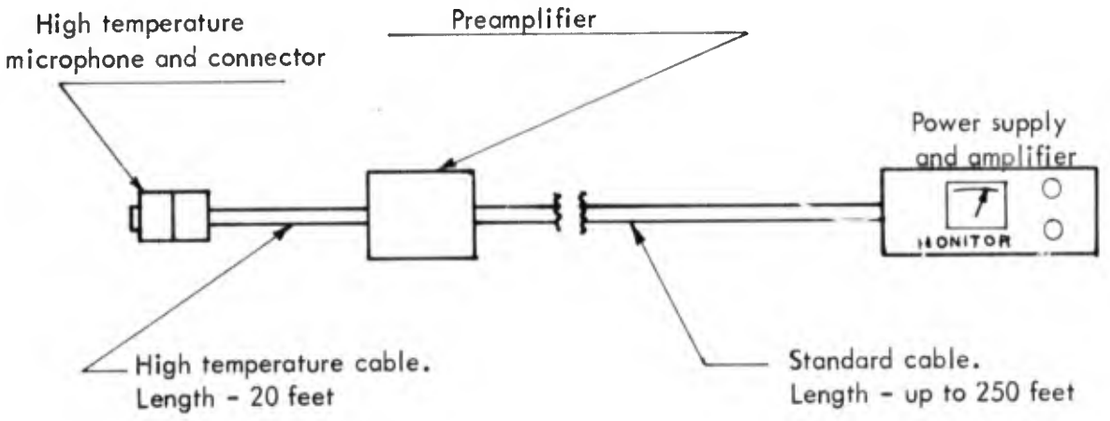

Figure 5. Block diagram of high temperature microphone system

The threshold noise spectrum for the preamplifier is shown in figure 8. The equivalent sound pressure levels shown in the ordinate are based on a microphone sensitivity of -86 db (re 1 volt/dyne/cm^2). Note that use of a high pass filter in the measurement system would significantly reduce the threshold noise. The maximum signal which the preamplifier will deliver to the amplifier is at least 30 volts, which is equivalent to the voltage output for a sound pressure level of about 190 db.

The power consumption of the preamplifier is 13 watts.

B. Amplifier

The circuit diagram for the amplifier is also shown in figure 6. The amplifier is heavily feedback-stabilized and has a voltage gain of approximately 40db. Final selection of this gain was determined by the sensitivity of the microphone. A two stage 90 db attenuator located at the input and output of the amplifier will allow attentuation to be added to the system in 10 db steps. Note that the first 50 db of attenuation is inserted at the amplifier output and additional attenuation, if needed, is inserted at the amplifier input. This scheme assures maximum signal-to-noise ratio for any attenuation desired. We note that the attenuator at the amplifier output is designed assuming a 5000 ohm load as indicated in the target specifications. Variation of this load would require a change in resistor values which make up this attenuator.
The design of the switch circuit will permit a single attenuator control and dial for the entire 90 db range. The 10 db steps will permit a system output voltage of 100 mv ±5 db for any sound pressure level in the range 100 to 190 db.

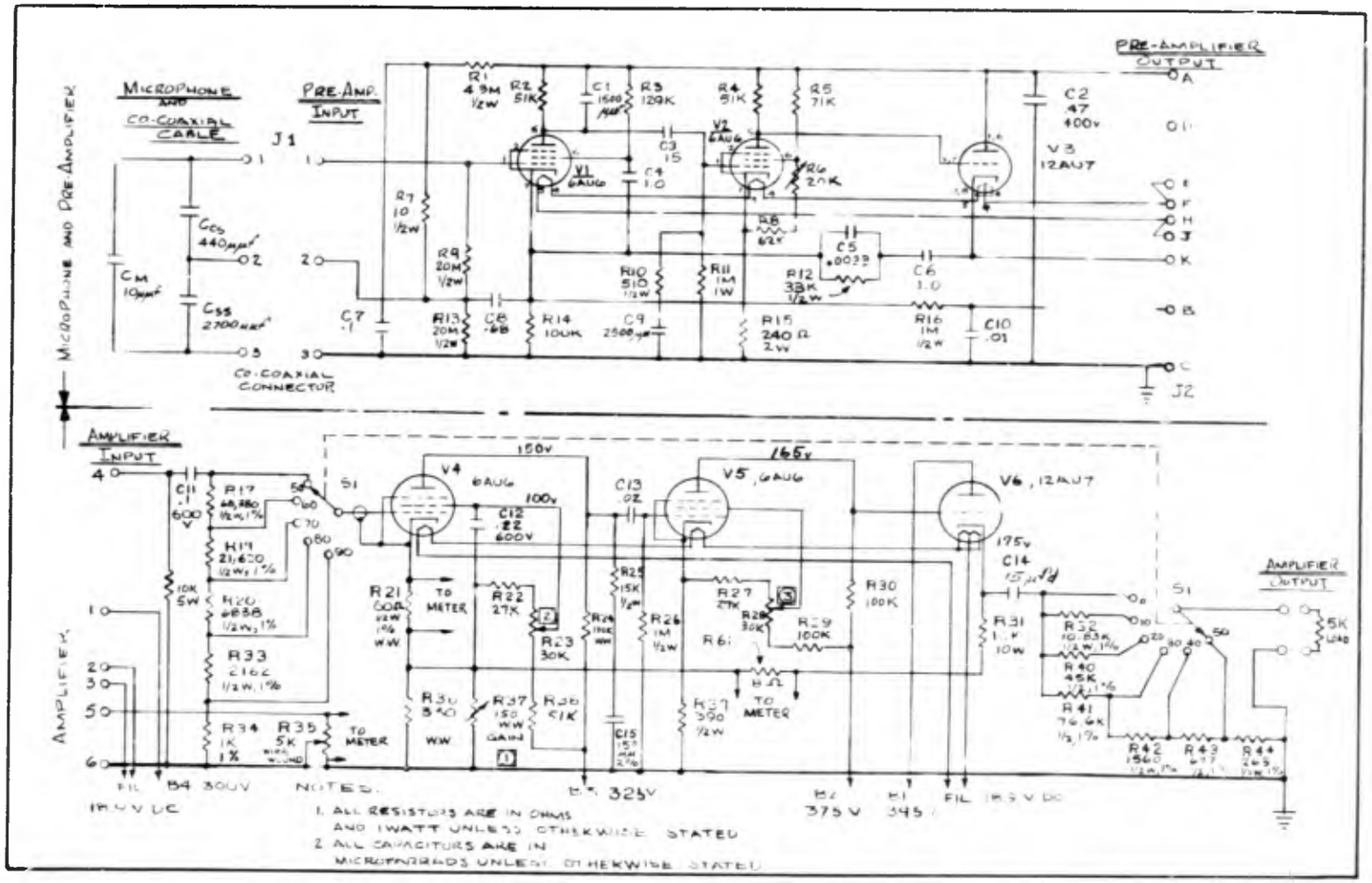

Figure 6. Circuit diagram for WEAL Type F Preamplifier and Type 100 F Condenser Microphone Complement.

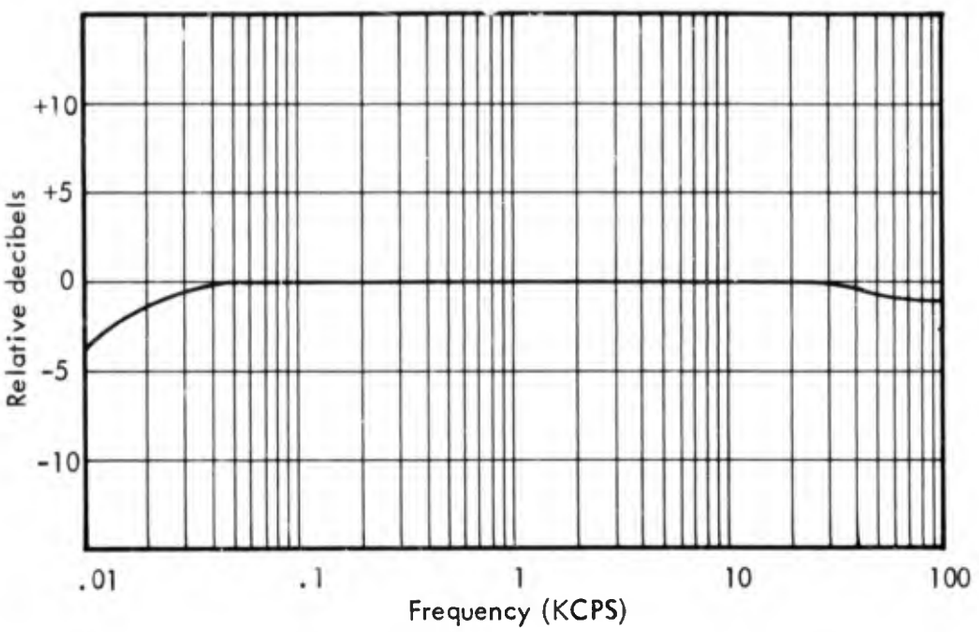

Figure 7. Measured frequency response for the WEAL Type F preamplifier including 20 feet of co-coaxial cable.

The threshold noise of the amplifier is on the order of 30 db less than that for the preamplifier and therefore is not an important factor in overall system noise.

Power consumption of the amplifier is about 13 watts.

The frequency response of the amplifier is flat within ±.5 db from 10 cps to 100 KCPS.

C. Power supply

The power package supplies all plate and filament voltages to the system. In addition, a highly stable polarizing voltage is supplied to the condenser microphone. All preamplifier and amplifier filaments are supplied with dc voltage for minimum system hum levels. Power consumption in the supply is 16 watts.

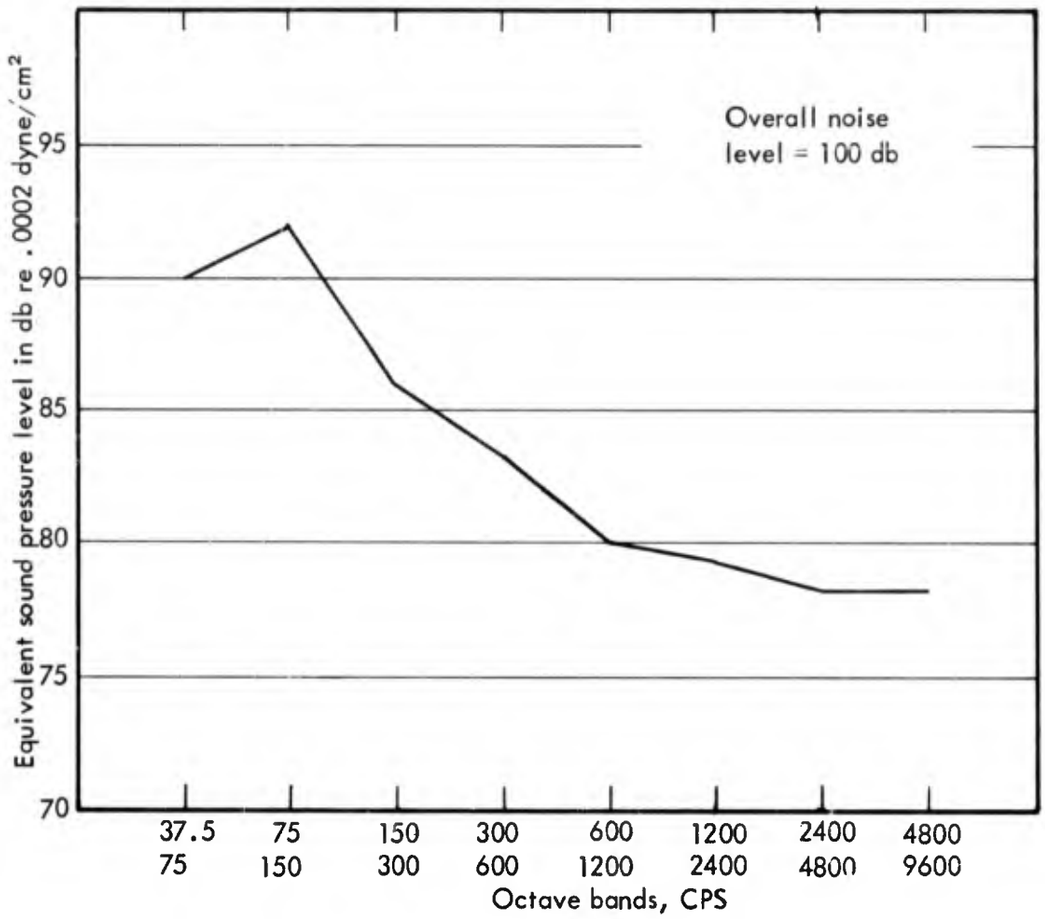

Figure 8. Measured threshold spectrum for the WEAL Type F preamplifier.

SECTION V

HEAT TRANSFER ELECTRICAL ANALOG STUDY

The development of the A-3 microphone was greatly facilitated by the utilization of an electrical analog of the heat flow characteristics of the microphone. It was deemed desirable in the program to utilize this technique. This section presents the concepts involved in the technique, as well as the results of the studies on the A-6 microphone and cable connector.

Before describing the design of the analog and its use, it is desirable at this point to review briefly the environment of the microphone in the boundary layer and to define clearly the source of heat energy, as well as the heat flow paths in the microphone and its surroundings.

The source of heat energy which affects the microphone temperatures is the turbulent boundary layer which exists at the boundary of a surface moving in a fluid medium. Heat is conducted away from or into the boundary layer due to temperature gradients, the direction of heat flow being dependent on the sign of the temperature gradient in the boundary layer. The discussion is facilitated by reference to figure 9, which shows typical temperature profiles in the fully developed turbulent flat-plate boundary layer for three different temperature gradients existing at the wall-to-fluid boundary. (Ref. 4) Curve "a" is the temperature profile when the wall is cooler than the adjacent portion of the boundary layer. In this case, heat flows from the boundary layer to the wall. Curve "c" is the profile when the wall temperature is greater than the boundary layer temperature, in which case heat flows from the wall to the boundary layer. Curve "b" is the steady state temperature profile in the boundary layer when the wall is thermally insulated from any heat sinks. Such a wall accepts heat energy from the boundary layer, with a subsequent rise in wall temperature until thermal balance is obtained between wall and boundary layer. The associated steady state wall temperature, by definition, is the recovery temperature and the profile "b" is the associated thermal gradient in the boundary layer. Note the zero temperature gradient at the wall-fluid interface for this steady state condition.

Of greatest interest in the present temperature analysis is the profile "a" of figure 9. In this case, the microphone assembly, mounting pad, and vehicle skin and interior are at a temperature below the recovery temperature so that heat flows from the boundary layer through the diaphragm to the microphone sub-assembly. However, the vehicle skin and interior temperature are in general transient, although their time constants are quite long relative to those of the diaphragm and microphone assembly. Thus, for long duration flights at a fixed speed and altitude, the overall vehicle temperatures will approach (asymptotically) recovery temperature, as will the microphone

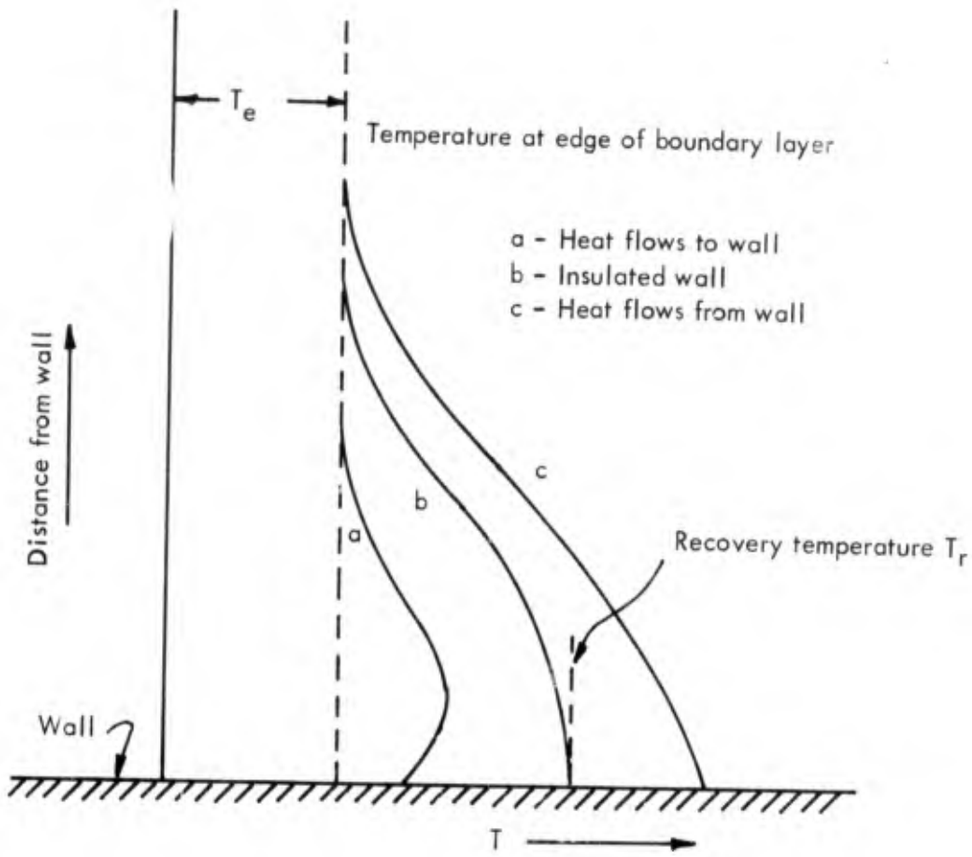

Figure 9. Schematic of boundary layer temperature profiles in a compressible viscous fluid. (From Ref. 4)

and diaphragm. In this case, profile "b" is appropriate. If after any such "heat soak" condition the vehicle quickly slows to a lower speed or climbs to a higher altitude, the vehicle temperature will be higher than the new and lower recovery temperature and profile "c" is appropriate.

In order to facilitate a clear understanding of the thermal conditions existing in the microphone, a schematic diagram of the heat flow paths is presented in figure 10. For purposes of this discussion, it is assumed that we are dealing with one dimensional heat flow so that radial heat flow from the diaphragm and backplate assembly is not indicated in the schematic. Under steady state conditions the necessary equations

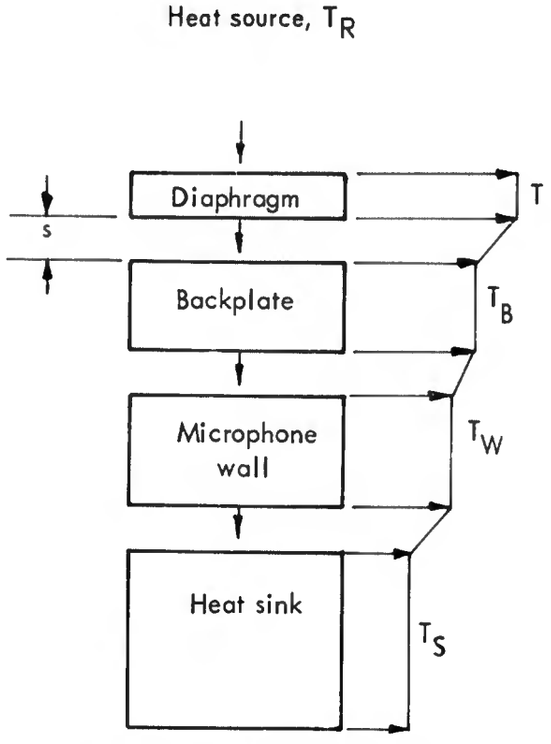

Figure 10. Schematic diagram of one dimensional heat flow paths in microphone assembly.

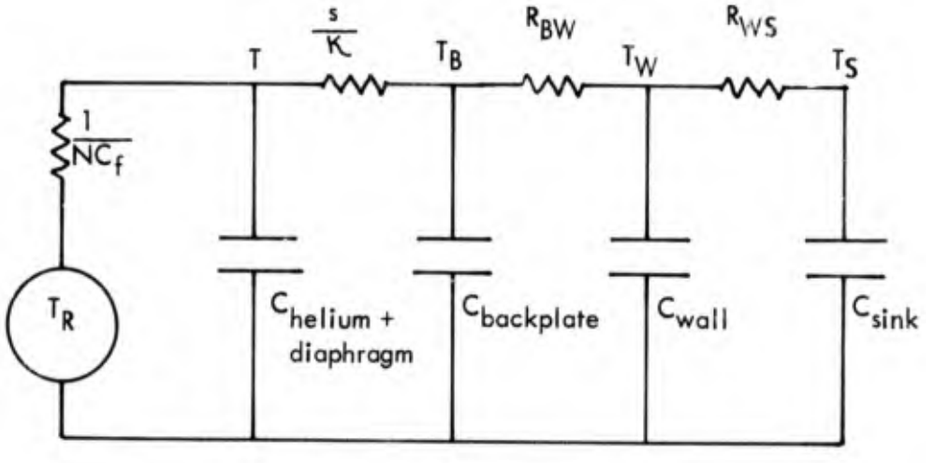

Figure 11. Analogous circuit diagram for the heat flow paths of figure 10.

defining the temperatures of the various microphone components are obtained from continuity of heat flow. These are

$$\dot{H} = NC_f (T_R - T) = \frac{K_s}{s} (T - T_B) = \frac{1}{R_{BW}} (T_B - T_W) \qquad (5)$$

$$+ \frac{1}{R_{WS}} (T_W - T_S)$$

All effects of radiation are neglected as these complicate the analyses considerably and are unimportant for diaphragm temperatures below 1000°F.

Equation 5 indicates a possibility of using an analogous electrical circuit to describe the heat flow condition in the microphone with the following analogies:

Heat flow rate ——— Current

Temperature difference — Voltage difference

Heat flow resistance —— Electrical resistance

The circuit diagram is shown in figure 11. The first three shunt capacitors have been included to account for the transient "charging up" of the diaphragm, diaphragm-to-backplate space, backplate and wall to their equilibrium temperatures. Thus, the thermal conditions in the microphone can be divided into three phases: the initial or transient phase which is represented by the diagram in figure 11, the steady state case which is represented by the diagram if the first three shunt capacitors are removed (this case is derived from equation 5 and, finally, the soak phase which is represented by the diagram if all the shunt capacitors are removed. The last condition corresponds to an open circuit in which case all temperatures are equal to recovery temperature.

It is clear from figure 11 that in the steady state case, knowledge of the thermal resistances in the boundary layer and microphone interior, as well as the recovery and heat sink temperatures, allows a determination of all microphone component temperatures. The values of recovery temperature T_R and the effective boundary layer resistance $1/NC_f$ can be calculated from flat plate zero degree angle of attack boundary layer theory while the microphone component thermal resistances can be calculated from the component dimensions and material thermal conductivities.

The discussion so far has been limited to a one dimensional lumped parameter system; however, the concepts are also applicable to a three dimensional "continuous" system which is the type of system actually used in the studies reported here. The term

"continuous" is not truly representative of the analog used here; however, a continuous system is for all practical purposes approached by dividing the microphone components into small segments and treating the small individual segments as lumped systems. Figure 12 shows the subdivision of the A-6 microphone and connector, and also indicates the temperature node points where temperatures can be measured. Each node point is connected to adjacent node points by a thermal resistance, hence the analog consists of a two dimensional array of resistances. The symmetry about the longitudinal axis of the microphone and connector allows a two-dimensional representation of the three dimensional heat flow.

Provision was made in the design of the analog to allow for variable spacing and hence variable resistance, between microphone diaphragm and backplate, i.e. between node pairs 1 - 11, 2 - 12, 3 - 13, 4 - 14, 5 - 15, 6 - 16, 8 - 17 and 9 - 18. The thermal resistance between the diaphragm and backplate plays a significant role in the ultimate temperatures of the diaphragm, hence variation in this thermal resistance due to either spacing changes or helium thermal conductivity changes must be taken into account. Thermal conductivity changes in the helium space between the guard ring and expander ring also necessitates the use of variable resistance between node pairs 22 - 23, 29 - 30, 36 - 38, 43 - 44, 50 - 52, 57 - 58, 66 - 67 and 75 - 76.

Note that the diaphragm has been segmented into ten areas so that the details of the diaphragm temperature profile could be obtained. The resistance between the boundary layer and the diaphragm are functions of both altitude and airflow velocity, hence these are variable in order that a large range of vehicle altitude and Mach number could be studied.

In actual use, the temperatures of all the node points are determined, once the input temperature (in our case the input temperature is the recovery temperature) and a reference temperature are chosen. The node point used as reference point is usually determined by the particular situation and can be arbitrarily chosen. It is customary to choose a node point whose temperature can be estimated with some accuracy. For example, if one or several of the node points of figure 12 were attached to a heat sink whose temperature was known or could be estimated, then these node points would be chosen as reference points and the reference temperature would be that of the heat sink. For the studies reported on here, two situations were studied. In the first, it was assumed that the base of the connector only was attached to a heat sink of constant temperature of 100°F. Node No. 103 was the reference point. In the second situation, it was assumed that the microphone wall up to node 109 and the entire connector wall were attached to a heat sink of temperature 100°F. In this case, nodes 103 to 109 were the reference points.

The results of these studies are presented in figures 13, 14, 16 and 17. Figures 13 and 14 present the resultant average diaphragm temperature contours for a large range

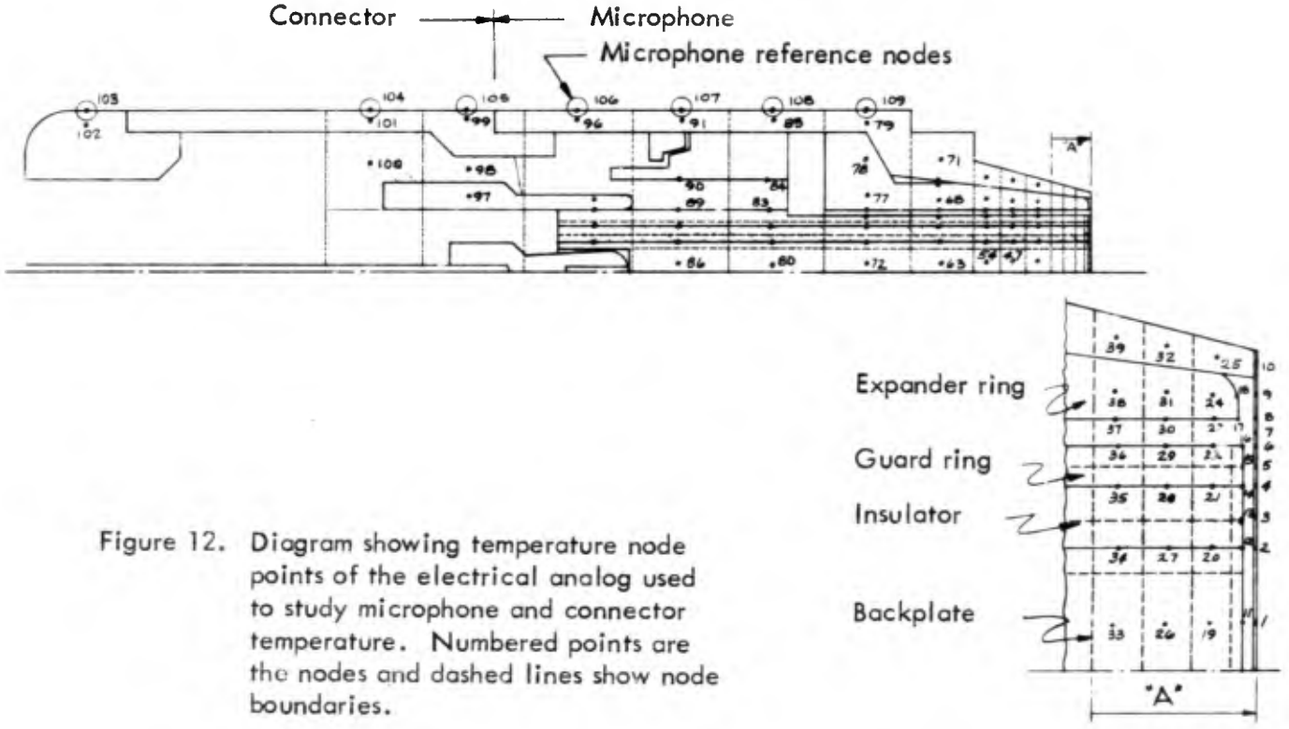

Figure 12. Diagram showing temperature node points of the electrical analog used to study microphone and connector temperature. Numbered points are the nodes and dashed lines show node boundaries.

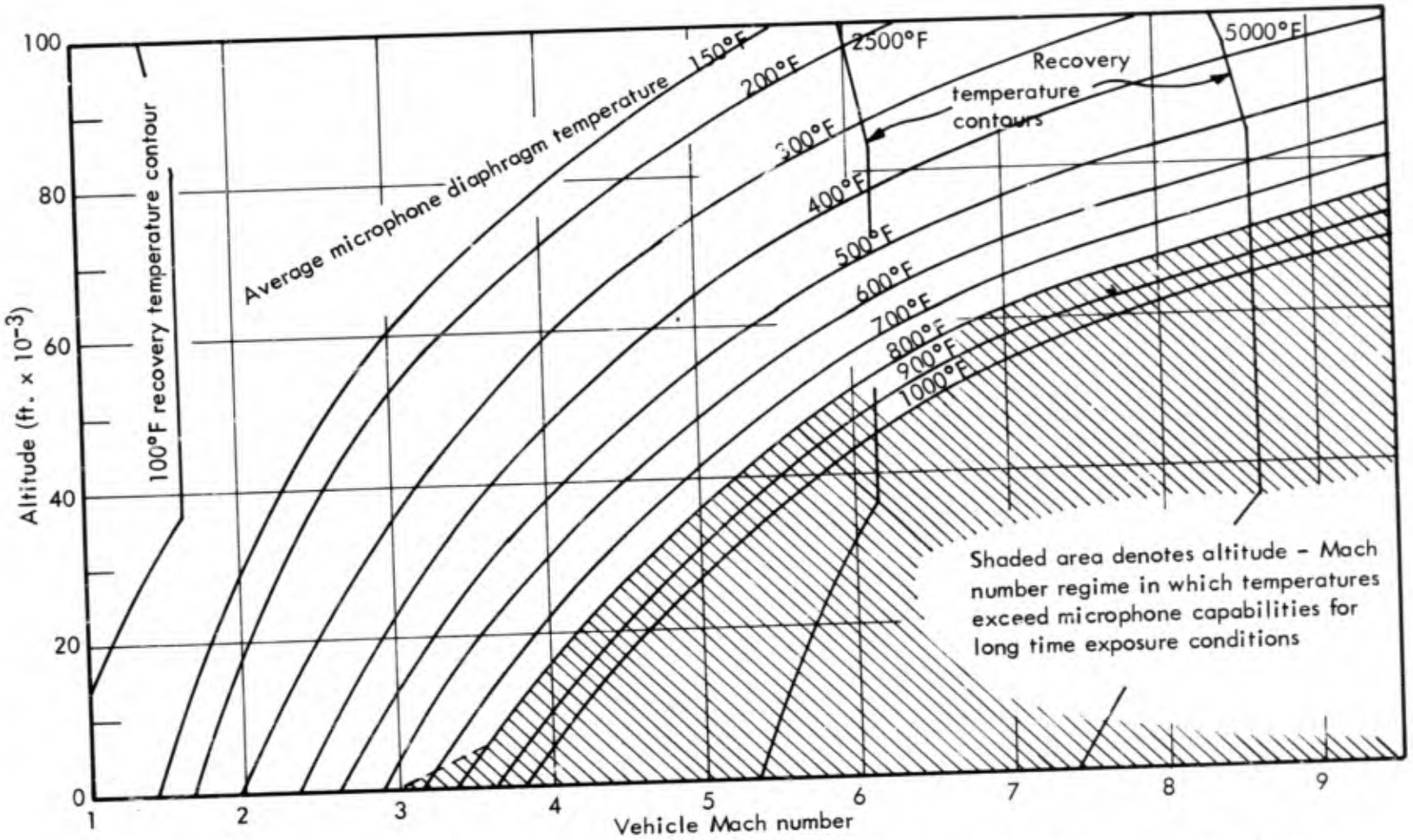

Figure 13. Measured average microphone diaphragm temperatures versus altitude and Mach number. Data obtained using an electrical analog of the microphone and aerothermodynamic parameters based on flat plate boundary layer theory, with node number 103 held at 100°F.

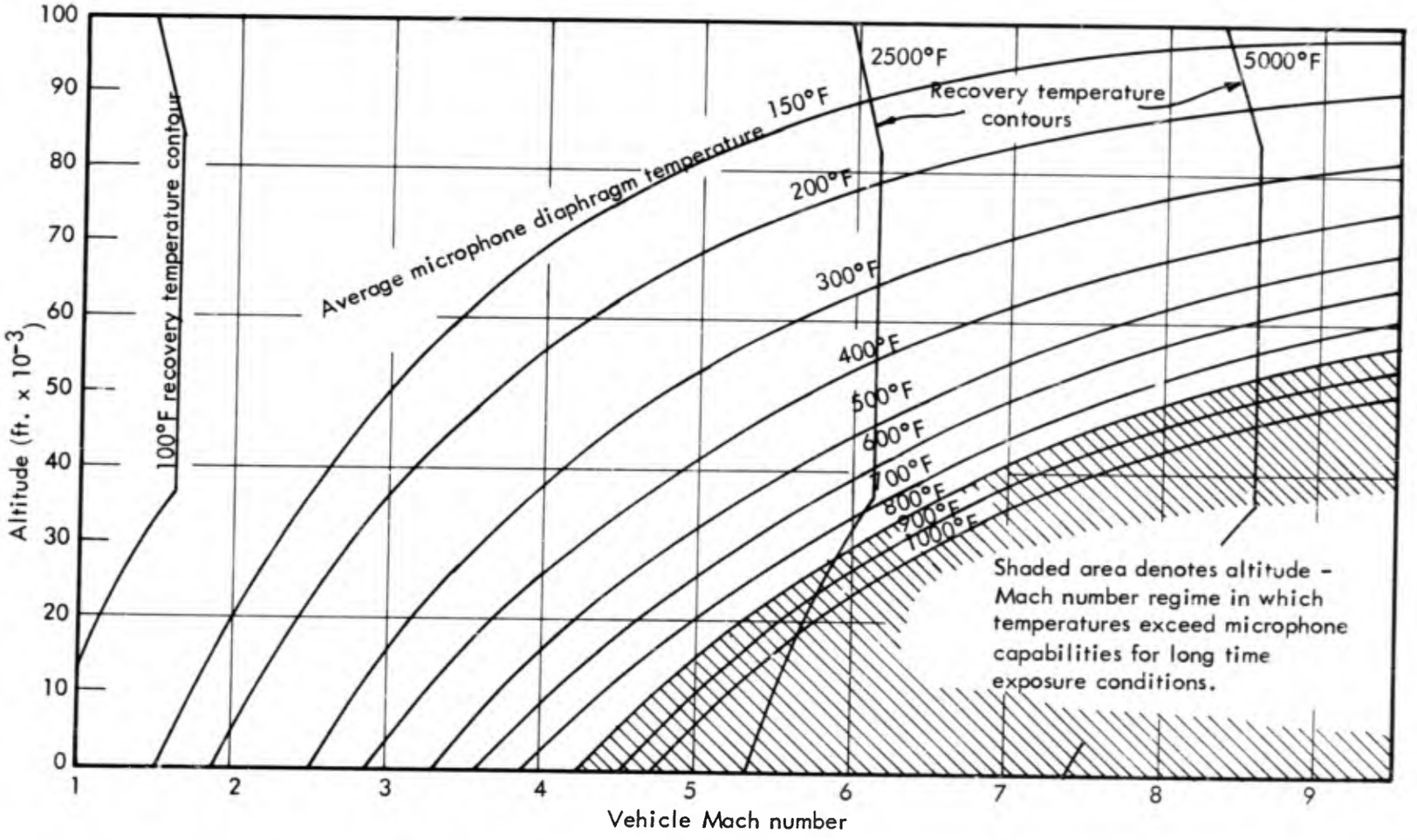

Figure 14. Measured average microphone diaphragm temperatures versus altitude and Mach number. Data obtained using an electrical analog of the microphone and aerothermodynamic parameters based on flat plate boundary layer theory with node numbers 103 to 109 held at 100°F.

of vehicle altitude and Mach number. As indicated in the figures, the low altitude high Mach number areas of the graphs for long time exposure would result in diaphragm temperatures beyond safe operating levels. The 800°F limiting curve is dictated by the yield strength versus temperature characteristics of the diaphragm material shown in figure 2. We note that the Pyroceram glass cement has a maximum service of temperature of 825°F; however, this material will always be at a somewhat lower temperature than the diaphragm. The 800°F temperature limit represents a 200°F increase in capability over the heat soak capability of the A-3 microphone. The dotted portion of the limiting curve of figure 13 near the sea level Mach 3 area results from a dangerously small backplate-to-diaphragm spacing which is the result of differential expansion. This limitation is not encountered for the case when the connector and microphone walls are held at 100°F.

We point out here the significant difference in the limiting 800°F curve of figure 13 and 14. The sea level maximum value of Mach number is increased from 3.0 to 4.25 when the microphone and connector wall are held to 100°F. This is, of course, expected, since the heat flow rate from diaphragm to heat sink is increased by this change. In actual use, it should be possible to design the mounting apparatus so that the 100°F or near 100°F temperature be maintained, hence the data of figure 14 is considered of practical importance.

The limitation at the high Mach number and low altitudes is not considered a serious limitation, since this area of exposure is encountered only rarely (if indeed possible). We note that re-entry vehicle exposure would probably not approach conditions represented by the shaded area. A high speed wind tunnel at sea level conditions might enter into this area, but present day "blowdown" wind tunnels would offer only short time exposures. Figure 15 shows some typical flight profiles for various vehicles. It is interesting to note that the microphone temperature limit of 800°F of figures 13 and 14 corresponds to recovery temperature values of up to 5000°F and greater for a very large altitude-Mach number area. The target specification of 2500°F recovery temperature is met except for a small area at low altitudes and high Mach numbers, which are unlikely to occur.

One of the objectives of this program was to design the backplate assembly so that a more uniform diaphragm temperature profile would result. It is felt that a substantial improvement has been accomplished in this area by the effective increase in heat flow cross-sectional area from diaphragm to the microphone interior. Typical diaphragm temperature profiles are shown in figures 16 and 17 for the two cases discussed above, showing maximum temperature variation in the profile of the order of 100°F for the condition of figure 17 and 30° for figure 16. We note that because of the increased temperature gradients in the microphone for the case when the microphone and connector walls are held to the 100°F temperature, the diaphragm

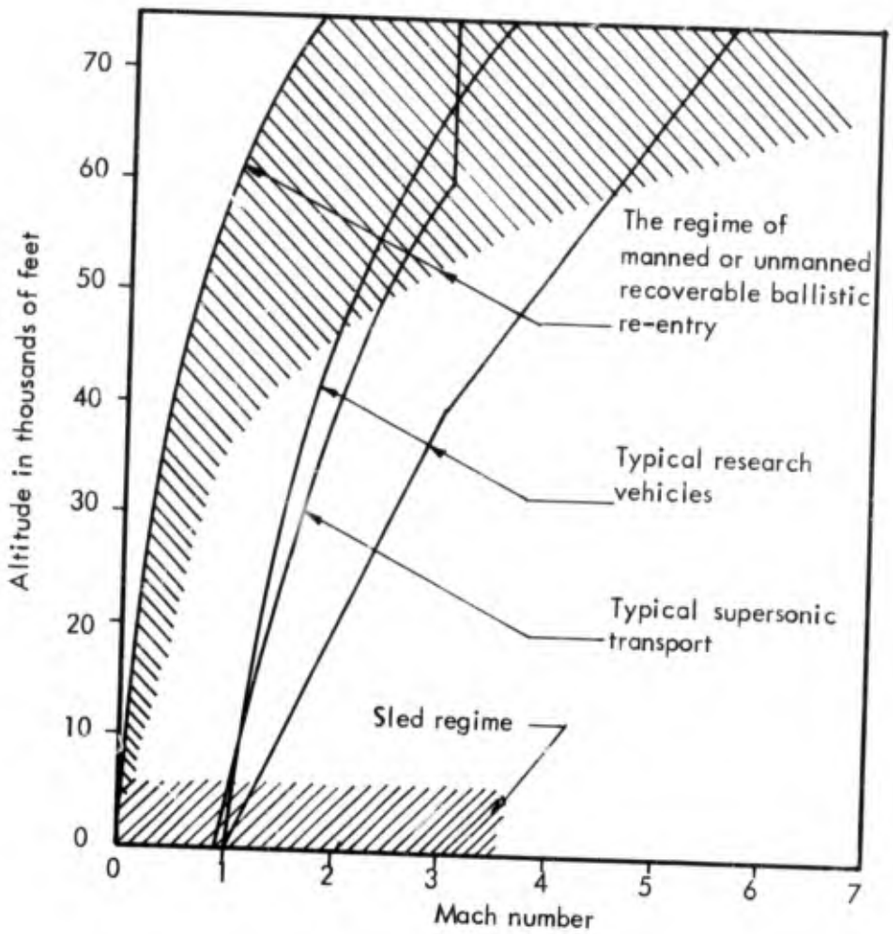

Figure 15. Typical altitude - Mach number flight profiles for ballistic re-entry, supersonic transport and sled vehicles.

temperature profile is not as uniform as for the case when only the connector base temperature is held constant. However, the uniformity is much better than for the A-3 microphone where variation in diaphragm temperatures were as high as 300°F in some cases. These observations are, of course, significant for the design of a heat sink for any particular application.

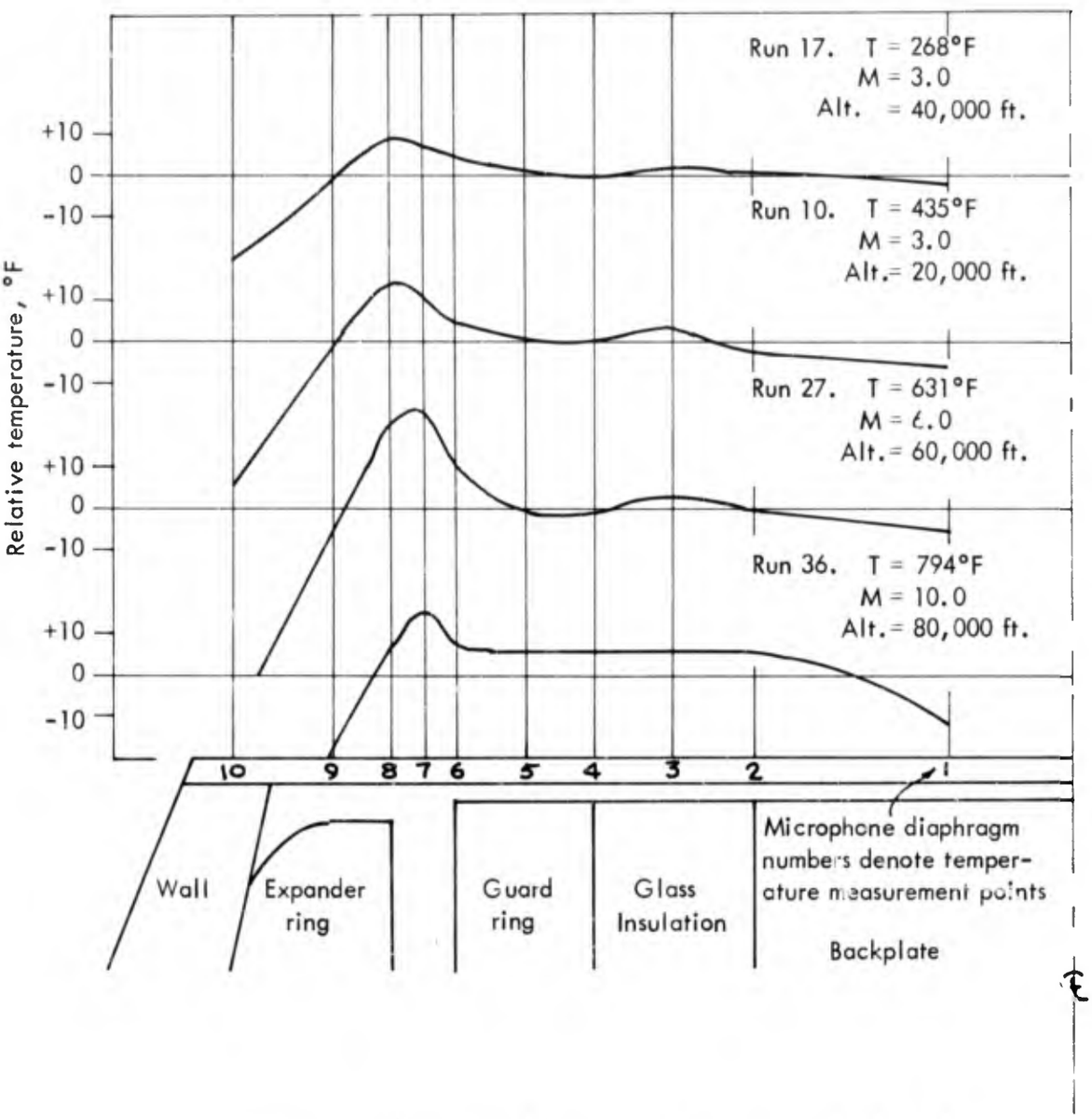

Figure 16. Typical measured microphone diaphragm temperature profiles using electrical analog when connector only is held to 100°F. The temperatures are plotted relative to the average diaphragm temperature.

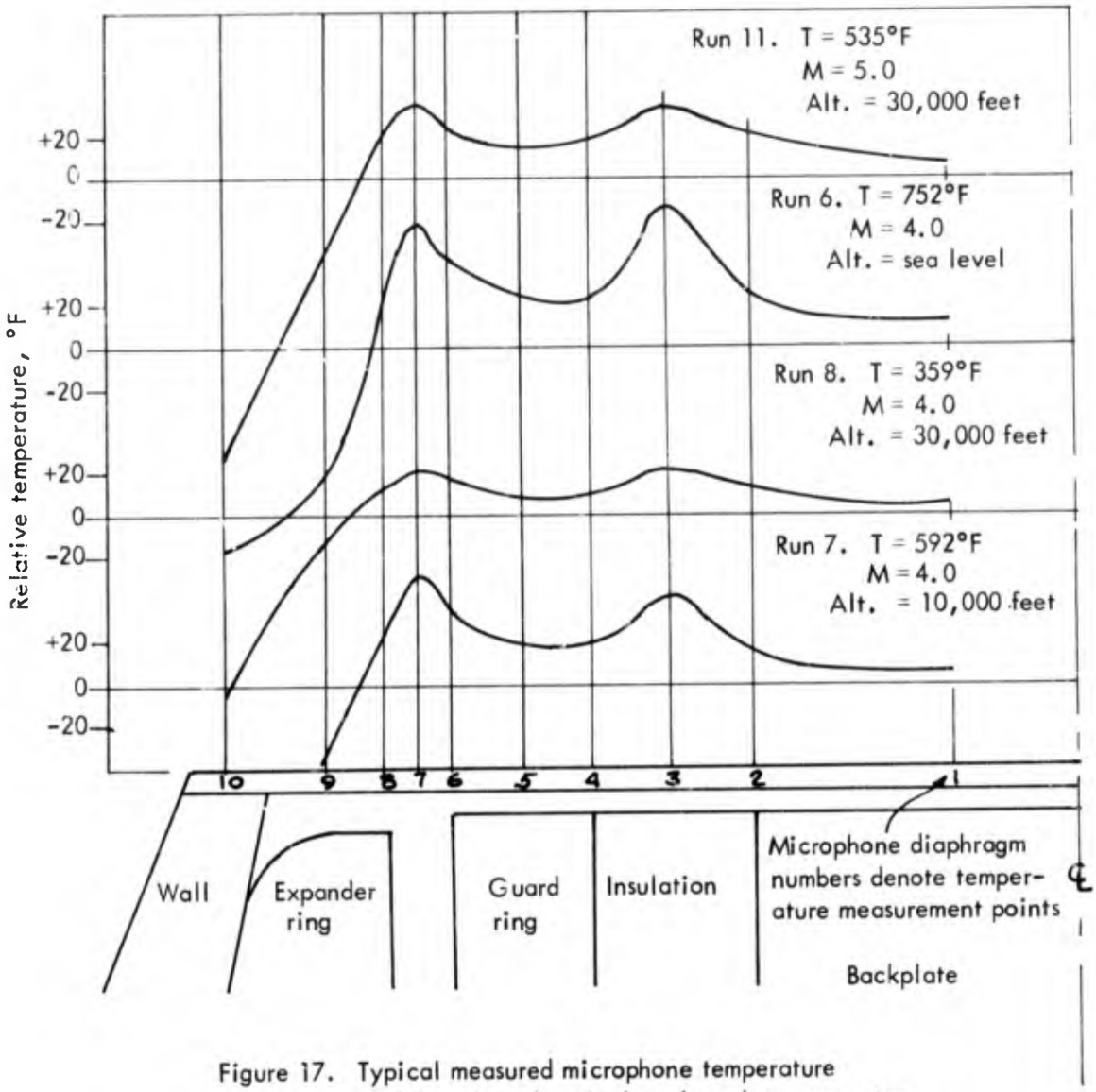

Figure 17. Typical measured microphone temperature profiles using electrical analog when connector and microphone walls are held to 100°F. The temperatures are plotted relative to the average diaphragm temperature.

SECTION VI

MICROPHONE SYSTEM CALIBRATIONS, TEST METHODS AND RESULTS

This section presents results of the calibrations which have been performed on the microphone systems. The method of calibration is also described.

In general, the results of the calibrations for the two microphone systems are quite similar; hence, in order to avoid needless repetition, typical data is presented rather than the data for each particular system. The reader is referred to the individual system calibration curves submitted if more precise information is desired.

A. Frequency Response and Absolute Calibration

The typical pressure frequency response and absolute calibration of the microphone system is shown in figure 18. The calibration is performed using an electrostatic actuator designed to thread on to the mounting threads located on the A-6 microphone. Essentially, the actuator is a metal grille placed close to and parallel to the microphone diaphragm. The actuator is electrically insulated from the diaphragm and a polarizing dc voltage (180 volts) is maintained between actuator and microphone diaphragm. An ac voltage superimposed on the dc voltage produces an alternating electrostatic force on the diaphragm which is independent of frequency. This alternating force on the diaphragm is fully equivalent to an alternating sound pressure acting on the diaphragm; hence, the frequency response is obtained by measuring system output versus frequency.

Also shown on the figure is the free field parallel incidence response for the microphone system.

The absolute scale on the ordinate of the curve in the figure is determined acoustically by a comparison calibration. This consists of comparing the output of the system with a standard microphone whose calibration is known when both are subjected to the same sound field. The standard microphone calibration is traceable to the National Bureau of Standards.

B. Sound Pressure Linearity

The sensitivity of a pressure transducer, which is defined as the ratio of output voltage to "input" pressure, is also a relation between the two parameters which determine the linear characteristics of a transducer. Hence, the constancy of the transducer sensitivity versus acoustic pressure, which is essential to accurate acoustic measurements, depends on the linear properties of the transducer.

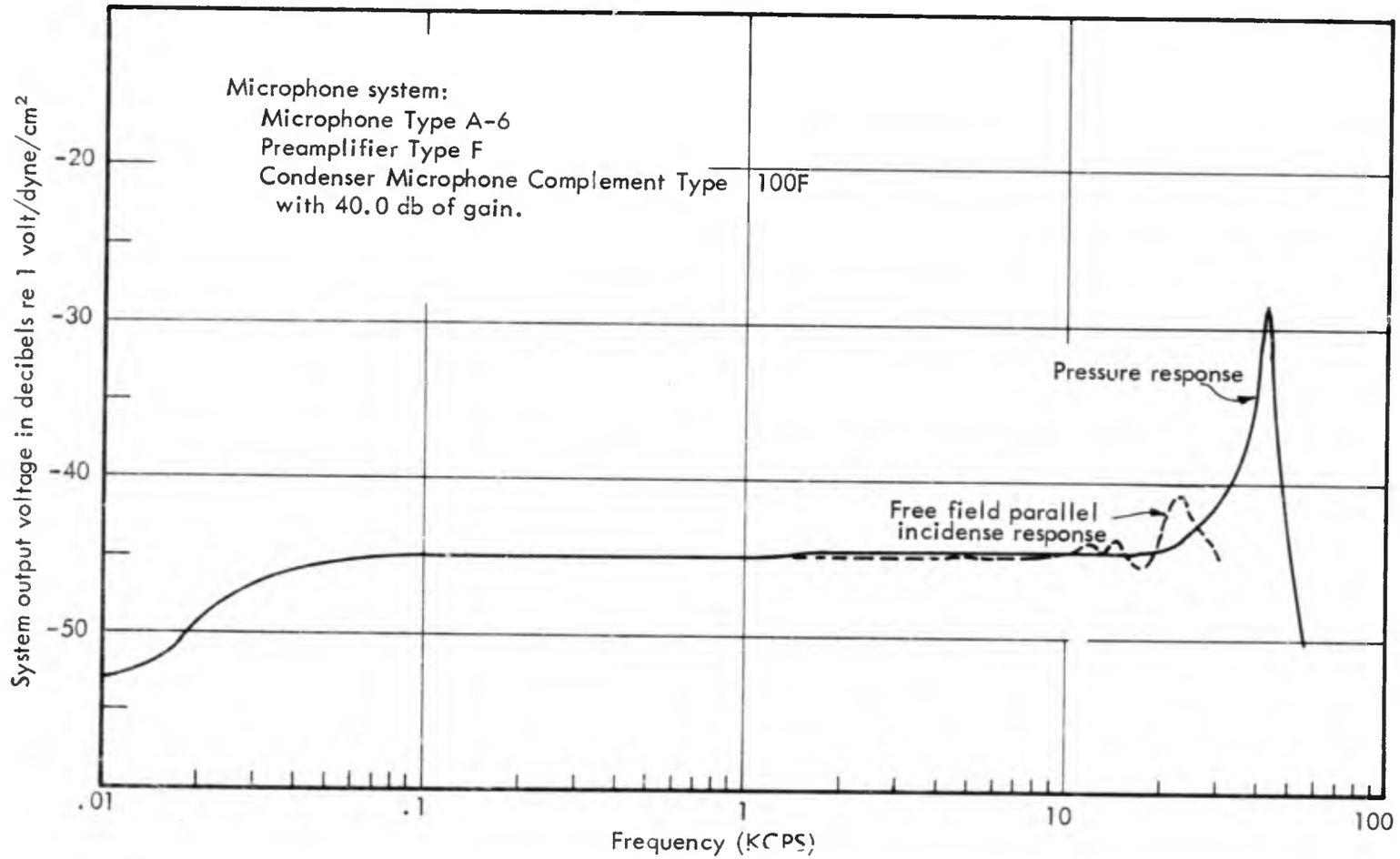

Figure 18. Typical microphone system calibration and frequency response.

There are two important properties of a pressure transducer which are affected by its non-linear properties. First, as mentioned above, the sensitivity of the microphone is constant only over the range of pressures for which the relation between output voltage and driving pressure is linear. Unless the relation between output voltage and driving pressure is known, errors will be present when measurements are performed during a transducer in its non-linear range. Even if this relation is known, measurements in the non-linear region become impractical because of the added complications which arise in data reduction. Secondly, a transducer which is operated in its non-linear region will produce a distorted signal. This distortion is evident in the spurious harmonics which are produced by the transducer.

The results of the linearity calibration on the microphone system are shown in figure 19. The data show that the systems are linear to ±.5 db in the range up to 160 db (re .0002 dyne/cm^2).

The linearity calibrations were performed using a resonant tube technique. Both the system microphone and a standard (which is known to be linear over the sound pressure level range of interest) are mounted at one end of a metal tube. The tube is driven acoustically by a loudspeaker placed at the opposite end of the tube. By exciting the tube at its fundamental natural frequency, very high sound pressure levels can be produced. As indicated in the figure, the linearity calibration was performed in 5 db increments from 110 db to 160 db, at a frequency of 123 cps.

C. Effect of Altitude on Operation

An increase in altitude is expected to cause a decrease in microphone sensitivity, due to the differential pressure across the diaphragm of a sealed condenser microphone. (See Appendix) The effect of this pressure differential is to move the diaphragm of the microphone away from the stationary backplate, thus decreasing microphone sensitivity.

Figure 20 shows schematically the system for measuring the change in microphone sensitivity with altitude. One method of creating a pressure differential across the microphone diaphragm, which is equivalent to the pressure differential at altitude, is to pressurize the cavity of the microphone. This was accomplished as shown in figure 20, by placing the microphone in the small pressure chamber with only the flush diaphragm exposed to the signal source. The back cavity of the microphone was not sealed during these tests so that pressure in the chamber also pressurized the back cavity. The chamber pressure was measured using a mercury manometer graduated in tenths of an inch.

A question arises concerning the validity of such a test in that the conditions here do not simulate identically the conditions at altitude. That is, at altitude the

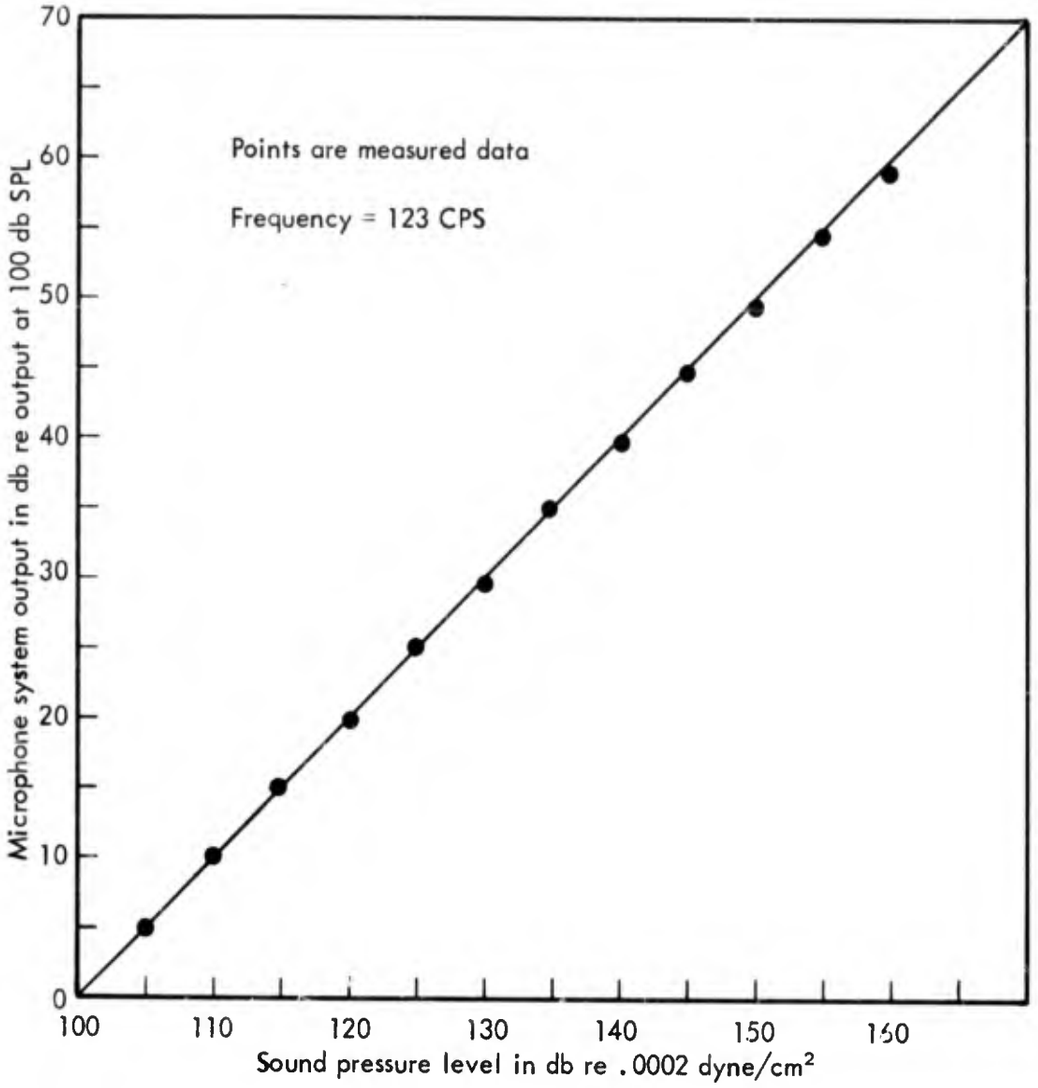

Figure 19. Linear relation between microphone system output and sound pressure level normalized to the output at 100 db SPL.

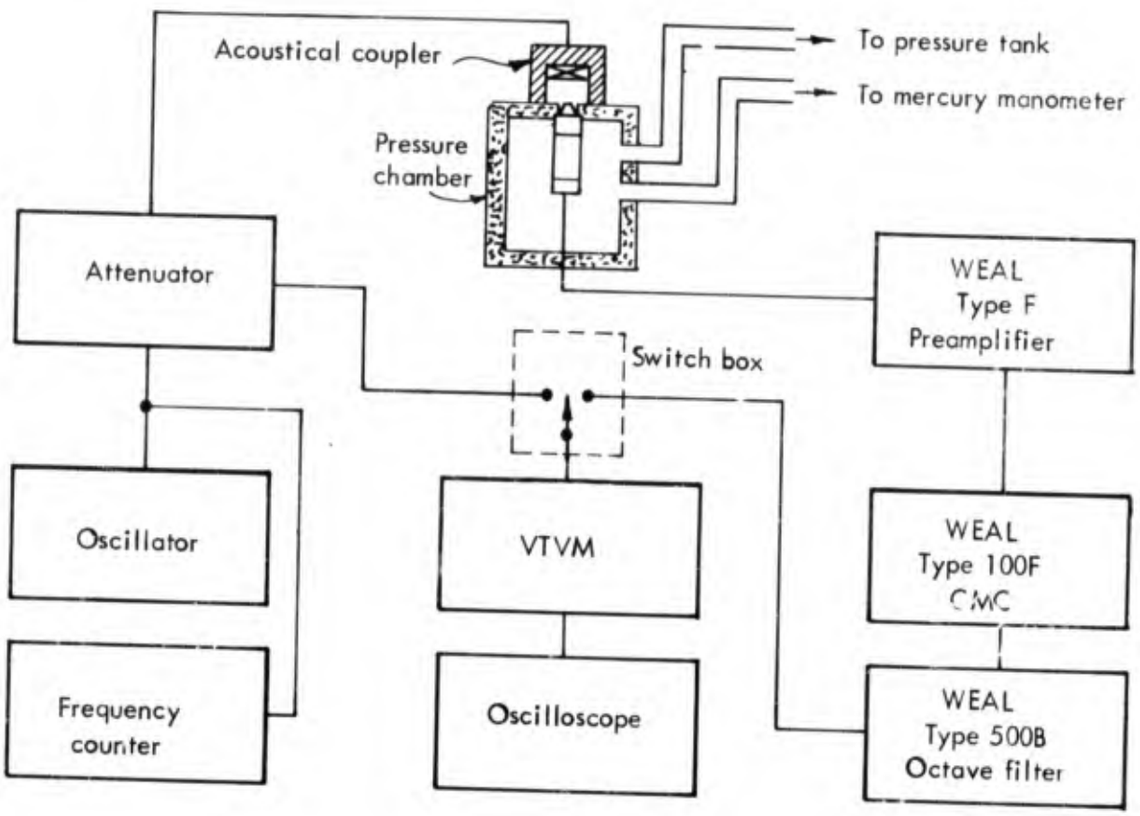

Figure 20. Block diagram of system used to measure the microphone response to altitude.

pressure inside a sealed microphone is one atmosphere, while during the test as outlined above, the pressure inside the microphone is two atmospheres, in order to achieve a one atmosphere pressure differential. Under these conditions it might be that we have changed the acoustical properties of the microphone cavity so that the simulation is not valid.

To answer this question the following experiment was performed: The microphone was placed inside the pressure chamber and the "acoustic" source in this case was an electrostatic actuator. With no pressure differential across the microphone diaphragm, the pressure was varied from one atmosphere to two atmospheres while monitoring the microphone output. The result of this experiment was that no difference in microphone

output was noted, indicating that the acoustical properties of the microphone cavity are not changed enough to affect the microphone response. This result validates the method used to obtain the microphone response to altitude.

The procedure for the test was as follows: With a steady 1 KCPS acoustic signal on the microphone diaphragm at normal pressure (i.e. no pressure differential), the output signal of the microphone was read on the VTVM and recorded. The pressure was then increased slightly and the output again recorded. This procedure was continued until a pressure differential of one atmosphere was reached. The procedure was then reversed by starting from one atmosphere pressure differential and decreasing pressure until a zero pressure differential was reached. No differences in microphone output change were noted on reversal of the procedure.

The results of the calibration versus altitude are shown in figure 21. Note that the curve flattens out at an altitude of about 130,000 ft. The response above 130,000 ft. is equal to that at 130,000 ft.

The effect of frequency on the response to an altitude change is seen on figure 21 where the results of a measurement using a 10 KCPS signal are included. It is seen that there is an apparent small effect at altitudes above 10,000 ft. where the loss in sensitivity is on the order of .2db higher. There is some question of the validity of this difference, since the experimental error is of the order of ±.2 db. In any case, it is safe to state that the effect is small.

D. Vibration Sensitivity

The vibration sensitivity measurement was performed by subjecting the microphone, microphone connector and a portion of the high temperature co-coaxial cable to a known sinusoidal vibration excitation and recording system output. The measurements revealed that the co-coaxial cable has greater response to vibration than the microphone. The signal levels from the system with and without the microphone connected showed little amplitude difference, and in addition, changes in signal output could be induced by movement of the cable near the microphone connector.

It is felt that the compliant glass insulation used in the cable for high temperature characteristics is responsible for the microphonic effects noted here. The relatively loose structural properties of the cable are also responsible for the variable output system signals for equivalent vibration amplitudes. This property made it difficult to obtain repeatability in the measurements. The data of figure 22 shows the results of the measurements in terms of equivalent sound pressure level for a one "g" vibration excitation level. The vertical bars in the figure denote the type of data variability which could be induced by movement of the cable relative to the connector base. This data, however, should be used with caution because of the nonrepeatable characteristic of the measurements.

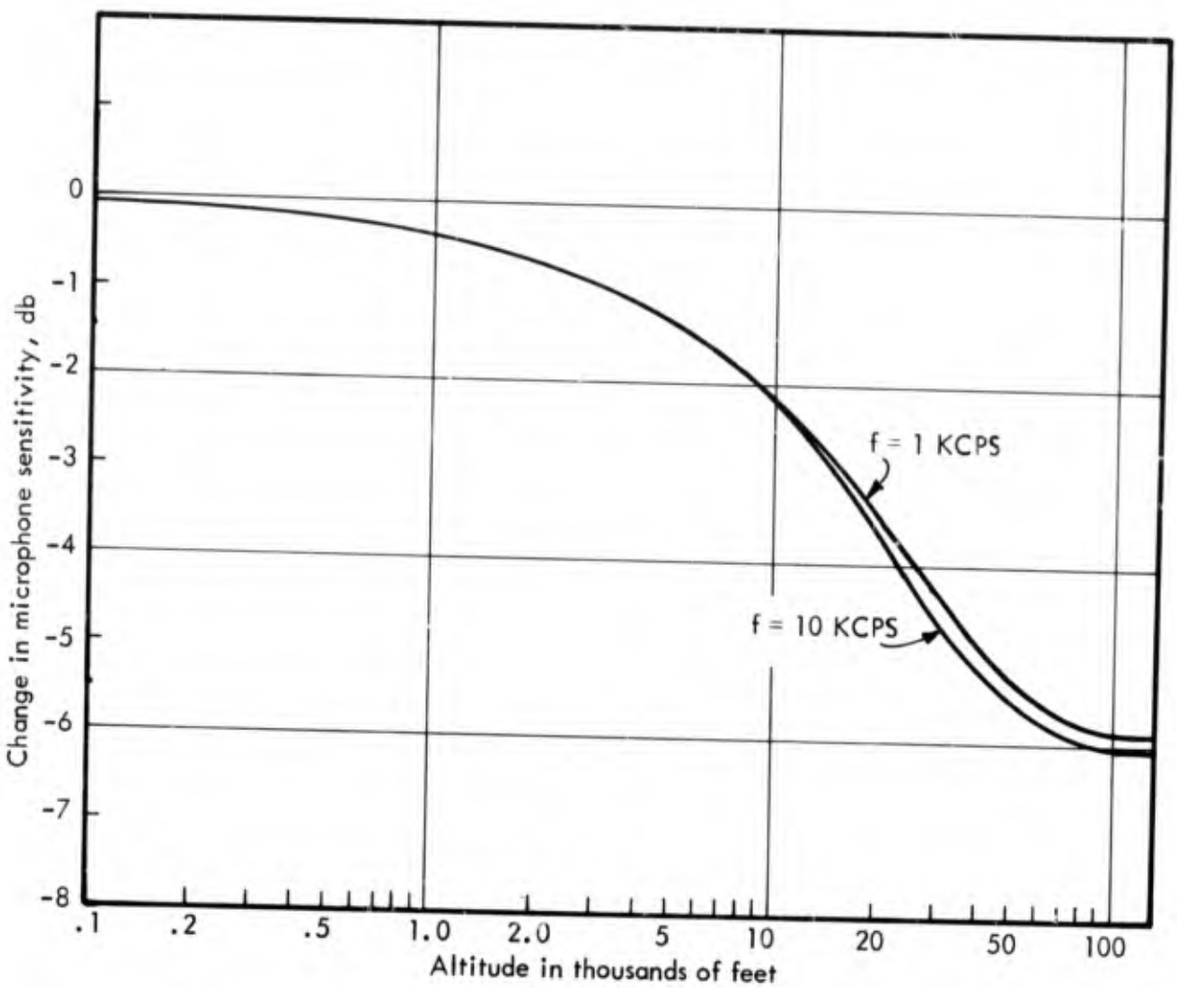

Figure 21. Typical response of a sealed A-6 condenser microphone to altitude for two different signal frequencies.

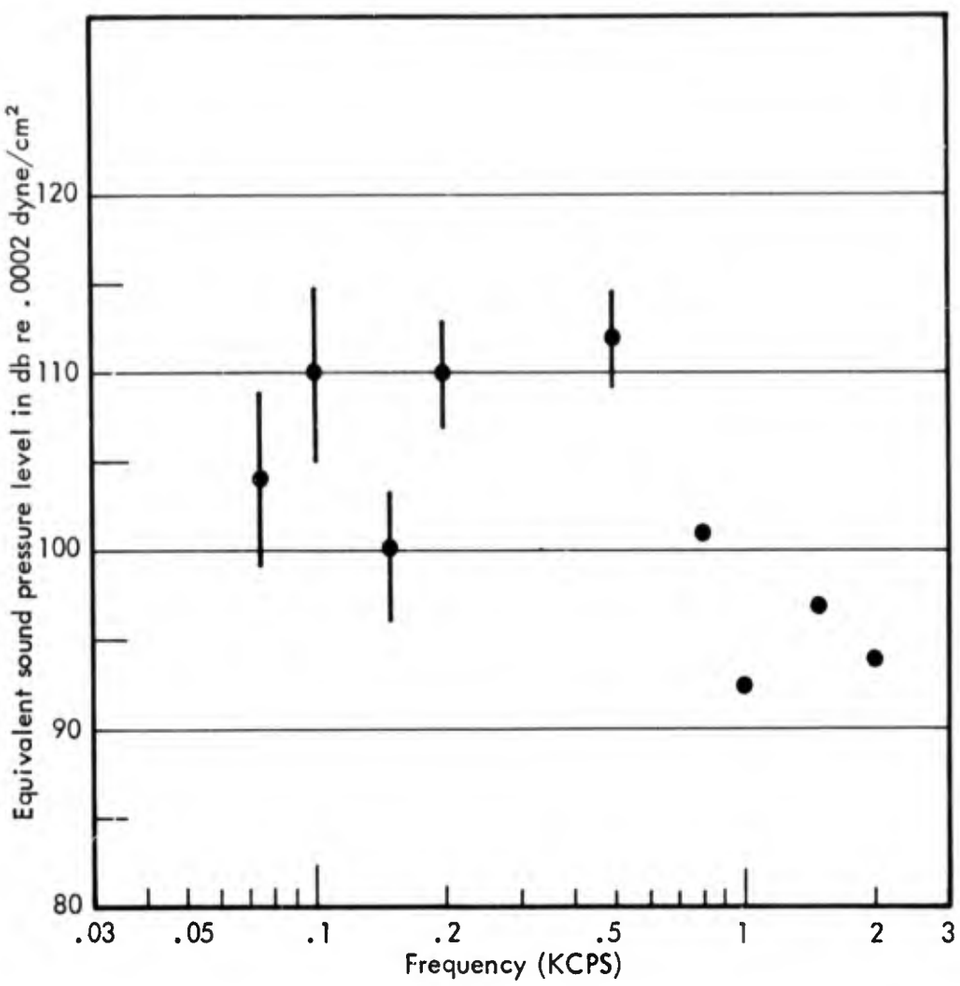

Figure 22. Measured response of microphone system to a one g acceleration level. The data points with vertical bars represent co-coaxial cable response rather than microphone response. The height of the bars represents variations in response due to cable movement. See text.

An improvement in the cable design could probably be achieved at the expense of high temperature characteristics and this problem will be investigated in future work.

E. Effect of Temperature on Operation

Before a description of the experiments to determine the effect of elevated temperatures is given, it is worthwhile to define the temperatures which are likely to be encountered. Theoretical calculations using flat plate boundary layer theory show that extremely high recovery temperatures are attained by a body moving in an air-stream at very high velocities. The recovery temperature is defined as that temperature which a thermally insulated body attains when the body remains in a high speed air-stream for a long enough period so that thermal equilibrium with the airstream is achieved. The two key phrases in this definition are "thermally insulated" and "thermal equilibrium."

A non-thermally insulated body will not reach recovery temperature until all heat sinks in thermal contact with the body also reach recovery temperature. As long as heat flows away from the hot body, recovery temperature is not attained. Obviously, to reduce the temperature of the body to tolerable levels, the heat flow resistance from the body should be minimized. The design of the WEAL A-6 microphone is based on this concept.

Calculations using flat plate theory and measurements using a thermal analog of the A-6 microphone show that for a "flight" condition of Mach 4.2 at sea level, where the recovery temperature would be 1600°F, the diaphragm temperature would reach 800°F. This same speed at 40,000 ft. would result in a diaphragm temperature of 300°F. (See figure 14) A speed of Mach 6.9 would be required to produce 800°F diaphragm temperature at 40,000 ft. These flight conditions are obviously extreme. Therefore, the 800°F diaphragm temperatures used in the following experiments are justified and they probably represent near maximum diaphragm temperatures in actual flight conditions.

The description of the experiments to determine the effect of temperature on the microphone system is facilitated by reference to figure 23. The pressure system shown in the figure was not used for the calibration described in this subsection. The idea of the experiment was to subject the diaphragm of the microphone to a known temperature and to measure any changes in microphone system output with temperature. A constant sound level was used to excite the microphone during the temperature variation. A monitor microphone was used to assure that the acoustic signal at the test microphone diaphragm was constant with time. The use of a probe microphone allowed the sound level at a distance of 3/8 inch from the test microphone diaphragm to be monitored at all temperature conditions. It was found that the sound level at the microphone diaphragm remained constant at all operating temperatures used in these measurements. Hence, any changes in test microphone output were due to the test microphone system and not due to variations in acoustic signal level. The test microphone output could be read off a VTVM

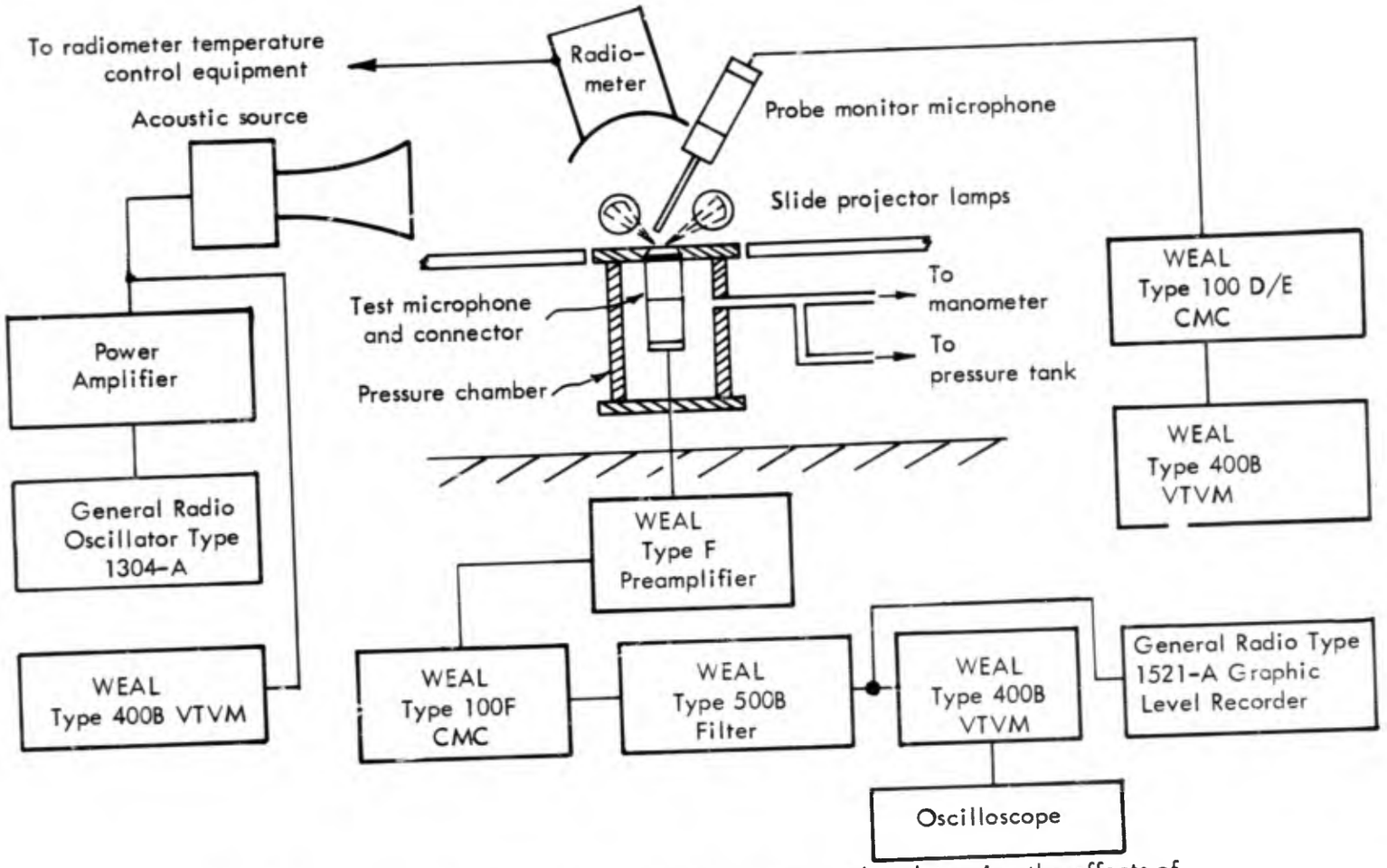

Figure 23. Block diagram of measurement equipment used to determine the effects of temperature and temperature-altitude on microphone system operation.

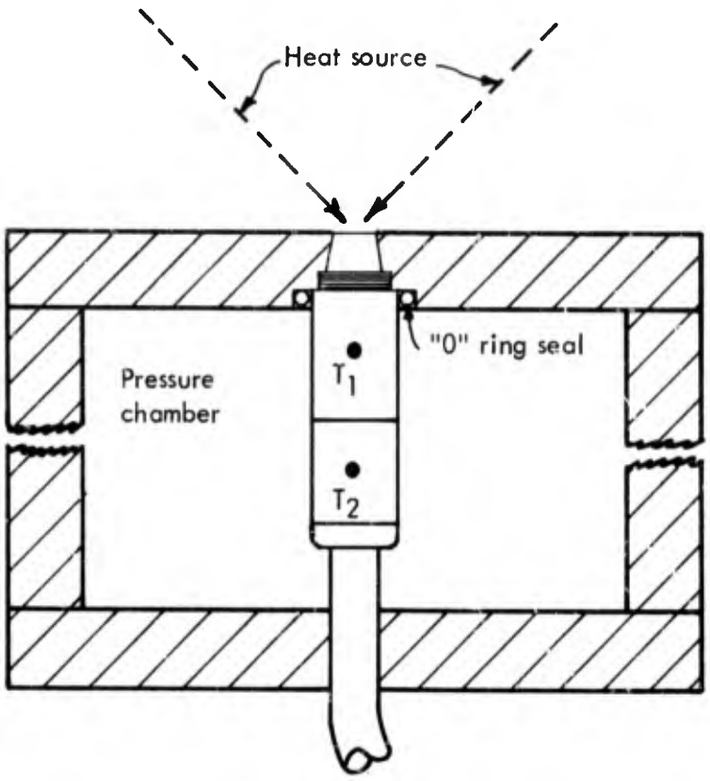

Figure 24. Schematic diagram showing the thermocouple locations used in the determination of temperature effects on microphone system operation.

graduated in decibels or a high speed level recorder.

The heat sources for this experiment were two General Electric DCA slide projector lamps placed close to the microphone diaphragm. These lamps incorporate a concave reflector which enables the lamps to focus their thermal energy over a very small area. In fact, it was possible to focus the heat from the lamps on the diaphragm of the microphone with very little heat immediately adjacent to the diaphragm. This scheme assures that any heat which gets to the other parts of the microphone travels through the microphone--a situation which simulates heating by the turbulent boundary layer.

The temperature of the diaphragm was measured with a Model R-401 radiometer manufactured by the Optitherm Industrial Co. This instrument allows one to measure the

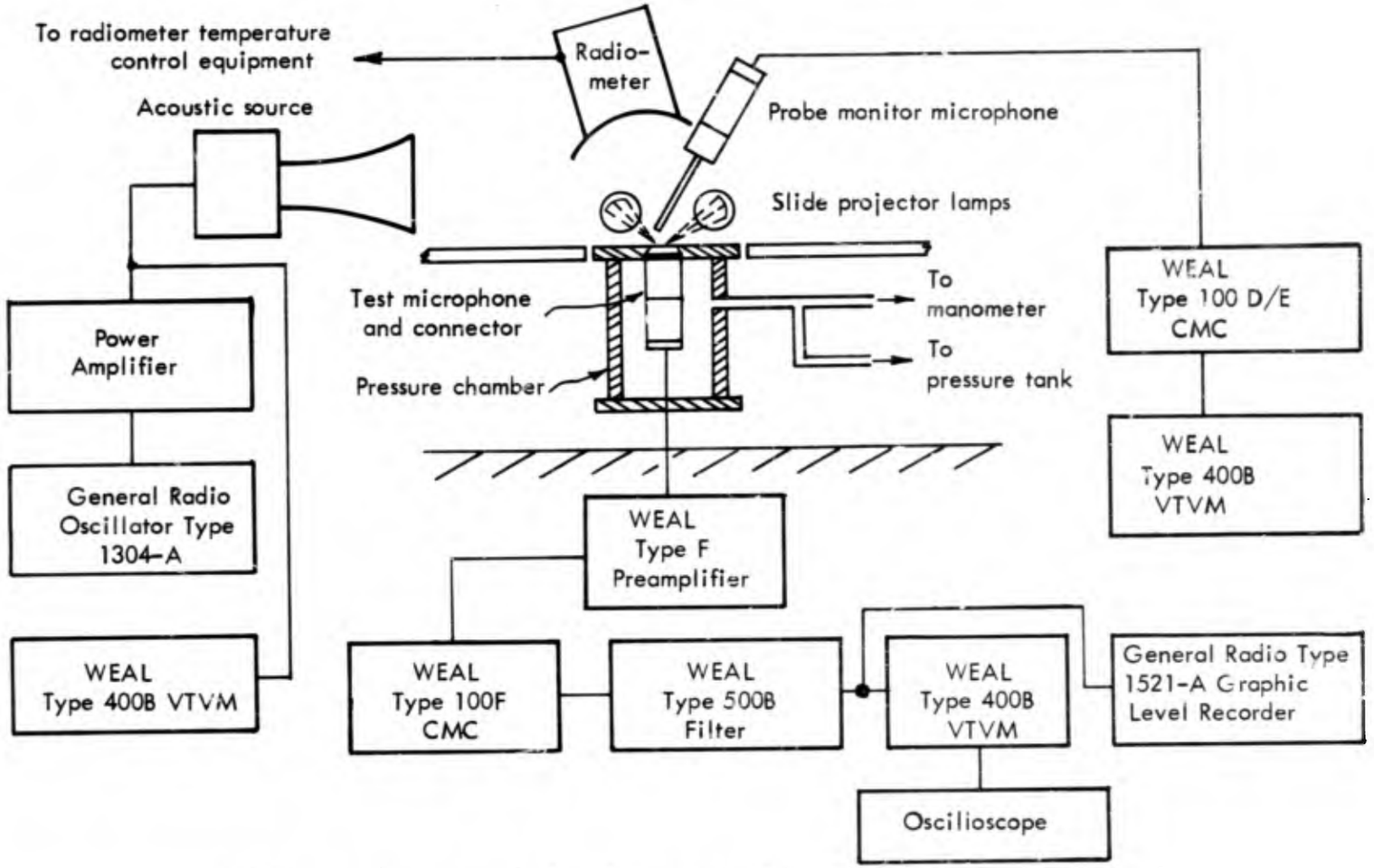

Figure 23. Block diagram of measurement equipment used to determine the effects of temperature and temperature-altitude on microphone system operation.

temperature of the diaphragm optically without having to contact the diaphragm. Because of the extremely small mass of the diaphragm, the use of a thermocouple to measure its temperature would lead to errors. In addition, the radiometer and its associated equipment was used to control the temperature of the microphone diaphragm by controlling the power supplied to the projector lamps. It was possible, for example, to bring the diaphragm to a known temperature for any desired time interval. The diaphragm temperature history was recorded on a strip chart recorder. In addition to measurement of the diaphragm temperature, the temperature at two other locations was measured using thermocouples. These thermocouples were used in conjunction with a Research, Inc., Model 4081 thermal reference junction and a Bristol strip chart recorder. The two thermocouple locations are shown in figure 24. With this experimental arrangement it was possible to obtain a time history of the three temperatures and the microphone output.

Two different types of experiments were performed to obtain the microphone response to diaphragm temperature. In the first experiment the microphone diaphragm was made to undergo a fairly rapid change in temperature so that the microphone response to a transient temperature could be studied. The results of this experiment are presented in figure 25. As seen in the figure, the response of the microphone follows quite closely the time history of the diaphragm temperature, except for a slight overshoot noted at the three minute point. This overshoot can be explained as follows: as the diaphragm temperature increases, its tendency to expand will reduce its tension and hence an increase in sensitivity is the result. We note that the decrease in diaphragm tension occurs because the wall to which it is attached, because of its relative mass, cannot follow the changes in diaphragm temperature, and hence will be cooler than the diaphragm. The difference in temperature between the diaphragm and wall is greatest during rapid changes in diaphragm temperature and therefore the microphone response changes will be greatest. When the diaphragm temperature is held constant after an initial increase, as is done in this experiment, the wall temperature tends to "catch up" with the diaphragm temperature and the response to temperature is decreased. This is the reason for the decreasing change in microphone sensitivity during the 3 to 12 minute period where the diaphragm temperature is held constant.

It is to be expected that the diaphragm temperature is not independent of the other parts of the microphone. In particular, its temperature is related to the temperature of the backplate because of its close thermal contact to the backplate. This fact is illustrated in figure 25. It was possible to control the decrease in diaphragm temperature to the point where the heat flow is reversed so that heat flows from the backplate to the diaphragm. After this the diaphragm temperature is controlled by the heat energy stored in the microphone interior. This is the reason for the relatively slow decrease in diaphragm temperature and hence slow change in microphone response after the 13 minute point. Note that after the 13 minute point the microphone sensitivity is less than the room temperature value. This indicates that the diaphragm temperature is less than the

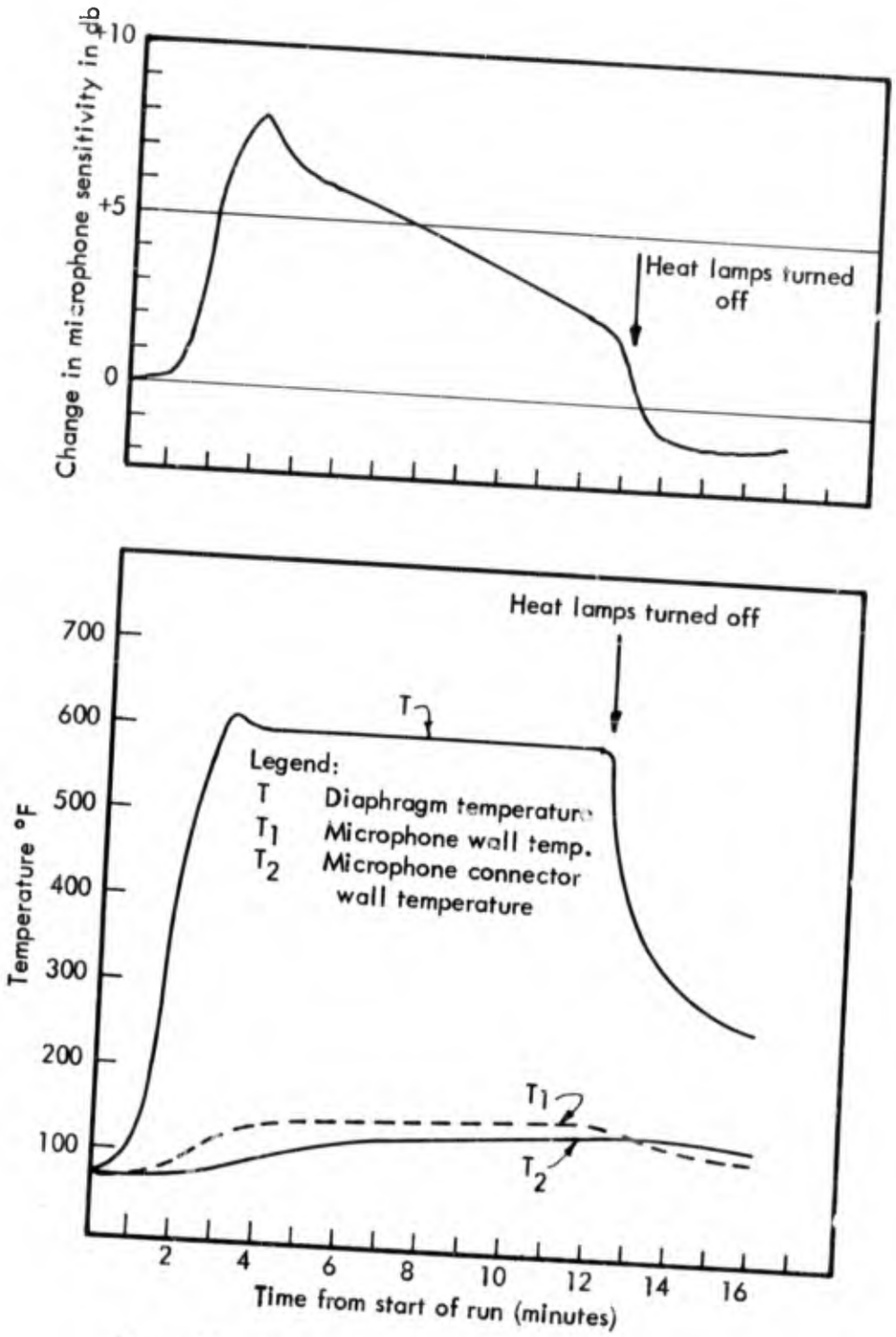

Figure 25. Measured time history of microphone sensitivity shown with the temperature time history at three microphone system locations. See figure 24.

wall temperature which is again lagging the diaphragm temperature, in which case its tension is increased and the result is a loss in sensitivity.

The above results serve to illustrate the dependence of the microphone response on the thermal conditions in the microphone. It also illustrates that in general temperature gradients exist in the microphone and hence calibrations of response to a "soak" temperature are not realistic.

In the second experiment the microphone response was monitored while the diaphragm temperature was increased from room temperature (normally 70°F) to various elevated temperatures. In each case the elevated temperature was held constant until equilibrium conditions were established. This was determined by noting when the microphone sensitivity change settled to a relatively constant value. The result of this sea level calibration is shown in figure 26.

F. Effect of a Combined Temperature and Altitude Environment on Operation

The ultimate use of the microphone system will be in a combined temperature-altitude environment and therefore a meaningful calibration should include these two environments simultaneously. The experimental apparatus shown in figure 23 was used to calibrate the microphone system in the required environment. The experimental method was essentially the same as that used for temperature calibration, except that the pressure apparatus was included to simulate an altitude environment.

The data which gives the response of the system to the combined environment was generated using the following method: starting with the microphone system at room temperature, the diaphragm was heated to a specified temperature and held there until the microphone response settled to a quasi equilibrium condition, then the pressure chamber was used to simulate several specified altitudes with the change in microphone system sensitivity noted for each altitude. This scheme produced data at a constant diaphragm temperature and several values of altitude. The method was repeated at several diaphragm temperature values. These included 70, 100, 200, 300, 400, 500, 700, and 800°F. The results of the calibration are shown in figure 26.

These results show that up to a diaphragm temperature of 700°F the shapes of the curves are somewhat similar except for a downward displacement caused by the loss in sensitivity at altitude. Or, in other words, the response to the combined altitude-temperature environment is altitude controlled. Actually, the results at sea level which show a rise above 500°F deviate slightly from the last statement. At diaphragm temperatures of 800°F there is a change in curve characteristic. At altitudes below and including 20,000 ft., the data tends toward an increase in sensitivity, indicating that the temperature effect predominates. Above 20,000 ft. the altitude effect controls the behavior and the response tends to decrease. This behavior is not surprising, since the

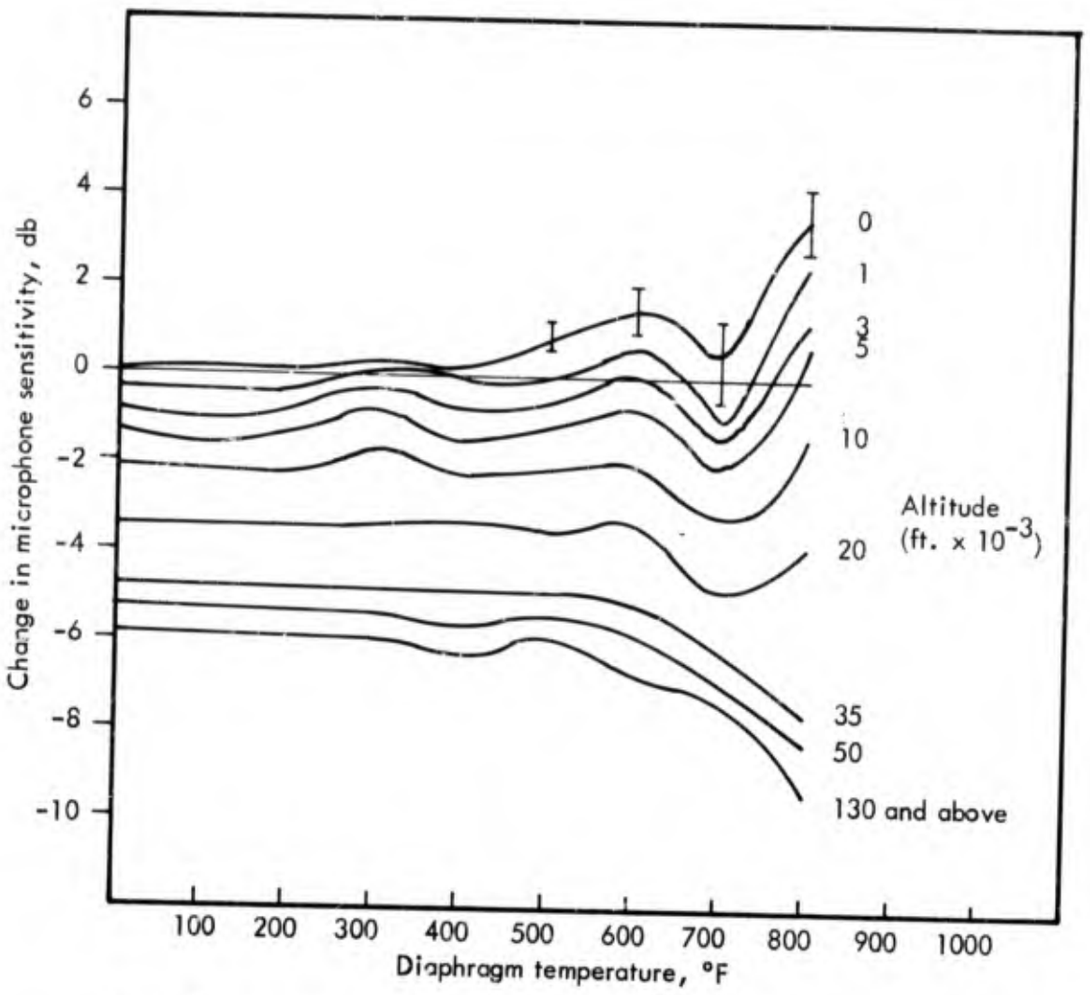

Figure 26. Typical sensitivity response versus temperature and altitude for a sealed WEAL Type A-6 condenser microphone.

altitude and temperature effects on the microphone response are of opposite sign and it would be expected that at some altitudes and temperatures one of these parameters will control the response.

The sea level data of figure 26 are indicated by vertical bars at temperatures of 500°F and above. This bar indicates the variability in the data over a period of about 10 minutes, which is the period of time required to make one run at constant diaphragm temperature. The upper end of the bar reflects the initial response reading and the lower end the final response reading. This variability, of course, corresponds to the decreasing

temperature differences between diaphragms and microphone walls, as discussed in the previous subsection and exemplified in figure 25. Given enough time, the response to temperature would tend toward zero or near zero, since the temperature gradients would be zero and, since the coefficients of thermal expansion of the microphone materials are quite similar.

The fact that the response to a combined altitude-temperature environment is primarily altitude controlled below diaphragm temperatures of 700°F can be beneficial. Reference to figures 13 and 14 shows that a very large area of altitude and Mach number is available to the microphone below diaphragm temperatures of 700°F. In addition, the data of figure 15 show that for practically all flight vehicles the vehicle speeds attain high Mach number only at high altitudes and the response of the A-6 microphone would be controlled by altitude effects. This is beneficial because it is always easier to predict or measure the altitude of a flight vehicle, and also easier to predict the response of a sealed microphone to altitude changes than it is to measure or predict temperatures on a vehicle surface, and hence microphone response to temperature.

The importance of the calibration curves of figure 26 lies in the ability to correct measured data for any flight condition within the boundaries of the data shown. We note here that the 130,000 ft. curve is applicable to all higher altitudes.

SECTION VII

CONCLUSIONS AND RECOMMENDATIONS FOR FUTURE RESEARCH

It is felt that the work in this program has resulted in a significant improvement in the overall measurement system and in particular, in the performance of the A-6 condenser microphone relative to the earlier A-3 microphone. The 800°F diaphragm temperature capability represents a 200°F increase over the earlier model and in a significant increase in altitude-Mach number range of flight conditions. The objectives of the program outlined in Section 1 of this report have been achieved.

We note that the proposed use of the system as an experimental laboratory piece of equipment led to concentration in the improvement of overall system performance for this type of application. For this reason, miniaturization of the system, particularly the electronics, was not considered of paramount importance. However, the concepts incorporated in the electronic design have, in fact, been specifically conceived with the prospect of miniaturization for use in airborne applications.

Some of the performance characteristics of the electronics do not meet the design objectives and in this respect we recommend further investigation. The research areas listed below are presented as a guide to future development.

A. Consideration should be given to transforming the present laboratory system to a transistorized airborne system. The advent of field effect transistors should allow design of small preamplifiers with high input impedance required for use with condenser microphones. The transistorized system would also be required to supply a stable polarizing voltage to the microphone.

B. The microphonic characteristics of the present high temperature cable is not desirable and should be eliminated. It is felt that this can be achieved with some compromise in cable temperature capability. This compromise is not serious, however, since the present cable capability of greater than 800°F is higher than need be. The use of a co-coaxial cable with an insulator of less compliance than the spun glass and with service temperature of about 600°F would meet present requirements. The use of silicone rubber as a cable insulator appears promising.

C. The method of combined temperature-altitude calibration used in this work proved adequate in this program. However, more sophisticated procedures could be developed. For example, it would be desirable to be able to program temperature and altitude environments to simulate actual dynamic flight conditions. In this way the transient heat conditions seen by the microphone could be simulated, and hence more accurate microphone response data could be obtained.

APPENDIX

THEORETICAL CONDENSER MICROPHONE PERFORMANCE CHARACTERISTICS

This appendix is a summary of theoretical work performed to obtain relations which could be used as guidelines in the design of the A-6 condenser microphone. In this report the relations derived have been used to determine condenser microphone parameters such as microphone sensitivity, diaphragm tension, diaphragm thickness, diaphragm-to-backplate spacing and other parameters associated with microphone overall response.

The derivation presented in part A of this appendix follows that of Ref. 5 with the exception that the derivation has been extended to account for a difference in radii of condenser microphone diaphragm and backplate. In addition, the low frequency sensitivity for a condenser microphone is derived taking into account the cavity stiffness behind the microphone diaphragm.

A. Frequency Response and Low Frequency Acoustic Sensitivity

The equation of motion for a driven membrane backed by a small volume is given as

$$\sigma \frac{\partial^2 \eta}{\partial t^2} = \tau \nabla^2 \eta + i\omega z \bar{\eta} + p e^{-i\omega t} \qquad \text{(A1)}$$

(Ref. 5)

where $\bar{\eta}$ is the average diaphragm displacement, which is given by the relation

$$\bar{\eta} = \frac{1}{\pi a_B^2} \int_0^{a_B} \eta r \, dr \int_0^{2\pi} d\phi = \frac{2}{a_B^2} \int_0^{a_B} \eta r \, dr \qquad \text{(A2)}$$

Note that the first integral in (A-2) is carried out over the interval 0 to a_B where a_B is the radius of the backplate. This is necessary since it is the average displacement of that part of the diaphragm which is over the backplate which is of interest.

A solution of (A-1) is

$$\eta = A\left[J_0\left(\frac{\omega r}{c}\right) - J_0\left(\frac{\omega a_0}{c}\right) \right] e^{-i\omega t} \qquad \text{(A3)}$$

where A is a constant to be determined and J_o is the well known Bessel function of zero order of the first kind. We note that equation (A-3) satisfies the boundary condition for a clamped circular membrane, since $\eta = 0$ for $r = a_D$

Substitution of (A-3) into (A-2) gives for $\bar{\eta}$

$$\bar{\eta} = \frac{2}{a_B^2}\int_0^{a_B}\left[A\left(J_o\left(\frac{\omega r}{c}\right) - J_o\left(\frac{\omega a_D}{c}\right)\right)e^{-i\omega t}\right] r\, dr$$

$$= \frac{2Ae^{-i\omega t}}{a_B}\left[\int_0^{a_B} r\, J_o\left(\frac{\omega r}{c}\right) dr - \frac{a_B^2}{2} J_o\left(\frac{\omega a_D}{c}\right)\right]$$

The integral term within the brackets can be written as

$$\int_0^{a_B} r\, J_o\left(\frac{\omega r}{c}\right) dr = \frac{c^2}{\omega^2}\int_0^{a_B} \frac{\omega r}{c} J_o\left(\frac{\omega r}{c}\right) d\left(\frac{\omega r}{c}\right)$$

$$= \frac{c}{\omega^2}\left[\frac{\omega r}{c} J_1\left(\frac{\omega r}{c}\right)\right]_0^{a_B} = \frac{c a_B}{\omega} J_1\left(\frac{\omega a_B}{c}\right)$$

Substituting this into the above, we get

$$\bar{\eta} = \frac{2Ae^{-i\omega t}}{a_B^2}\left[\frac{c a_B}{\omega} J_1\left(\frac{\omega a_B}{c}\right) - \frac{a_B^2}{2} J_o\left(\frac{\omega a_D}{c}\right)\right]$$

or

$$\bar{\eta} = Ae^{-i\omega t}\left[\frac{2c}{\omega a_B} J_1\left(\frac{\omega a_B}{c}\right) - J_o\left(\frac{\omega a_D}{c}\right)\right] \qquad \text{(A4)}$$

We note that the expression for $\bar{\eta}$ when $a_B = a_D$ is

$$\bar{\eta}_{a_B = a_D} = Ae^{-i\omega t} J_2\left(\frac{\omega a_D}{c}\right)$$

which agrees with the value for $\overline{\eta}$ given in Ref. 5, where it is assumed that the radius of the backplate and diaphragm are equal.

Equation (A-4) is the relation which expresses the average diaphragm displacement for a microphone with a backplate whose radius is a_B. In order to utilize this expression, it is now necessary to evaluate the constant A.

This is done by substituting equation (A-3) and (A-4) into equation (A-1). Performing this substitution and solving for A results in the relation

$$A = \frac{p}{\sigma\omega^2 J_0(\mu) - i\omega Z\left[\frac{2}{\gamma} J_1(\gamma) - J_0(\mu)\right] + \frac{\tau\omega^2}{2c^2} J_0(\beta) - \frac{\tau\omega^2}{2c^2} J_2(\beta) + \frac{\tau\omega}{\pi c} J_1(\beta) - \sigma\omega^2 J_0(\beta)}$$

where $\mu = \frac{\omega a_D}{c}$, $\beta = \frac{\omega\pi}{c}$, $\gamma = \frac{\omega a_B}{c}$

This relation for A can be simplified somewhat. It turns out that the sum of the last four terms in the denominator are identically equal to zero and this is shown as follows: recall that $c^2 = \frac{\tau}{\sigma}$. Therefore, these four terms can be written as

$$\frac{\sigma\omega^2}{2} J_0(\beta) - \frac{\sigma\omega^2}{2} J_2(\beta) + \frac{\tau\omega}{\pi c} J_1(\beta) - \sigma\omega^2 J_0(\beta)$$

multiplying through by $\frac{\pi c}{\tau\omega}$ and re-arranging terms, we get for the sum

$$J_1(\beta) - \tfrac{1}{2}\beta J_0(\beta) - \tfrac{1}{2}\beta J_2(\beta)$$

but this group of terms sums to zero when we invoke the recurrence formula (Ref. 6).

$$J_1(\beta) = \tfrac{1}{2}\beta\left[J_0(\beta) + J_2(\beta)\right]$$

The relation for A can then be written

$$A = \frac{p\frac{\pi c}{\tau\omega}}{\frac{\pi c}{\tau\omega}\sigma\omega^2 J_0(\mu) - i\frac{\pi c}{\tau\omega}\omega Z\left[\frac{2}{\gamma} J_1(\gamma) - J_0(\mu)\right]}$$

which upon further manipulation, becomes

$$A = \frac{\frac{p a_0^2}{T \mu^2}}{J_0(\mu) + \frac{\zeta}{i\mu}\left[\frac{2}{\gamma} J_1(\gamma) - J_0(\mu)\right]} \tag{A5}$$

where

$$\zeta \equiv \theta - i\chi = \frac{a_0}{\sigma c}(R - iX) = \frac{a_0}{\sigma c} z \tag{A6}$$

and $z = R - iX$ is the specific acoustic impedance acting on both sides of the diaphragm and ζ is an impedance ratio.
Substitution of (A-5) into (A-4) gives for the average diaphragm displacement

$$\bar{\eta} = \frac{\frac{p a_0^2}{T \mu^2}\left[\frac{2}{\gamma} J_1(\gamma) - J_0(\mu)\right] e^{-i\omega t}}{J_0(\mu) + \frac{\zeta}{i\mu}\left[\frac{2}{\gamma} J_1(\gamma) - J_0(\mu)\right]} \tag{A7}$$

Equation (A-7) can be put into a more useful form by manipulation of the term

$$\frac{e^{-i\omega t}}{J_0(\mu) + \frac{\zeta}{i\mu}\left[\frac{2}{\gamma} J_1(\gamma) - J_0(\mu)\right]}$$

which can be shown to be equal to

$$\frac{e^{-i(\omega t - \Omega)}}{\left[\left(J_0(\mu) - \frac{\chi}{\mu} J(\gamma, \mu)\right)^2 + \left(\frac{\theta}{\mu}\right)^2 J^2(\gamma, \mu)\right]^{1/2}}$$

where we define

$$J(\gamma,\mu) \equiv \frac{2}{\gamma} J_1(\gamma) - J_0(\mu) \tag{A8}$$

and

$$\text{TAN}\,\Omega = \frac{\theta\, J(\gamma,\mu)}{\mu J_0(\mu) - \chi J(\gamma,\mu)} \tag{A9}$$

Substituting this into (A-7) above, we get

$$\bar{\eta} = \frac{p a_D^2}{\tau \mu^2} \quad \frac{J(\gamma,\mu)\, e^{-i(\omega t - \Omega)}}{\left[\left(J_0(\mu) - \frac{\chi}{\mu} J(\gamma,\mu)\right)^2 + \left(\frac{\theta}{\mu}\right)^2 J^2(\gamma,\mu)\right]^{1/2}}$$

or

$$\bar{\eta} = \frac{p a_D^2}{\tau} H(\gamma,\mu)\, e^{-i(\omega t - \Omega)} \tag{A10}$$

where

$$H(\gamma,\mu) = \frac{J(\gamma,\mu)}{\mu^2\left[\left(J_0(\mu) - \frac{\chi}{\mu} J(\gamma,\mu)\right)^2 + \left(\frac{\theta}{\mu}\right)^2 J^2(\gamma,\mu)\right]^{1/2}} \tag{A11}$$

Equation (A-10) which shows that the average diaphragm displacement $\bar{\eta}$ is proportional to the applied pressure p and inversely proportional to the tension τ is also the relation which gives the frequency response of the diaphragm displacement through the frequency parameter $H(\gamma,\mu)$. As shown in equation (A-11), if the specific acoustic

Impedance (z) as seen by the diaphragm, is known, then in principle the average displacement $\bar{\eta}$ versus frequency can be obtained. In practice, however, the value of z is quite complex. For example, if one considers the factors which make up the specific acoustic impedance z, we find that for a condenser microphone there are three which are important. These are the radiation impedance for the microphone diaphragm, the impedance behind the microphone diaphragm which is due to a small film of air between the microphone diaphragm and the backplate, and the impedance of the cavity behind the microphone diaphragm. The first two of these factors are complex functions of frequency and use of these parameters in equation (A-11) would be a task for a computer. The impedance due to the microphone cavity is relatively simple in terms of incorporation into equation (A-11). In fact, it turns out to be useful in the calculation of the low frequency sensitivity of a condenser microphone where the radiation impedance and the thin air film impedance can be neglected. This is shown later on in this section.

The relationship between the voltage output of a condenser microphone and the average diaphragm displacement $\bar{\eta}$ is obtained as follows:

Consider a condenser microphone with backplate radius a_B, distance between diaphragm and backplate s and polarizing voltage E_o. In the usual circuitry, the input resistance of the amplifier associated with the condenser microphone is very large, with the result that charge on the microphone remains constant with time. This fact results in a fluctuating voltage across the microphone capacitance when fluctuations in the position of the diaphragm relative to the backplate occur.

If C be the capacity of a condenser microphone, E the voltage across it and Q the total charge, then we have simply

$$E = \frac{Q}{C} \tag{A12}$$

and $$dE = -\frac{Q}{C^2}\, dC + \frac{1}{C} dQ$$

but for this case dQ = 0 and therefore

$$dE = -\frac{Q}{C^2}\, dC \tag{A13}$$

where dE is the change in voltage across the microphone due to a change in capacitance dC. But

$$C = \frac{kS}{s}$$

and

$$dC = \frac{-kS}{s^2}\, ds \tag{A14}$$

where k = constant

S = backplate area

substituting (A-14) into (A-13) we get

$$dE = \frac{E_o\, ds}{s} \tag{A15}$$

But the quantity dE is equivalent to the microphone output voltage and the quantity ds is equivalent to the average diaphragm displacement $\bar{\eta}$. Letting $dE \equiv e$ we get therefore that the magnitude of the output voltage is

$$e = \frac{E_o \bar{\eta}}{s} \qquad \text{or}$$

$$e = \frac{E_o p Q_o^2}{s T} H(\gamma, \mu)\, e^{-i(\omega t - \Omega)} \tag{A16}$$

Finally, defining the microphone sensitivity (M) the usual way, we obtain the general expression for the sensitivity of a condenser microphone:

$$M = \frac{e}{p} = \frac{E_o Q_o^2}{s T} H(\gamma, \mu)\, e^{-i(\omega t - \Omega)} \tag{A17}$$

The low frequency value of M can now be obtained by evaluation H(γ, μ) when γ and μ go to zero (i.e. when the frequency goes to zero). In the following calculation it is assumed that the reactive part of the specific acoustic impedance z is due only to the stiffness of the cavity behind the microphone diaphragm, since the reactive part of the radiation impedance at low frequencies is small (Ref.5) and the work of Ref. 7 has shown that the stiffness due to the air film between the microphone diaphragm and the backplate is zero at zero frequency.

The acoustic impedance of the microphone cavity Z_A is given by

$$Z_A = \frac{i \rho c_A^2}{\omega V} \tag{A18}$$

which when transformed to specific acoustic impedance and using the relation of equation (A-6), becomes

$$X = -\frac{\pi a_0^2 \rho c_A^2}{\omega V}$$

Therefore,

$$\chi = -\frac{\rho c_A^2 \pi a_D^4}{\tau V \mu} = -\frac{K}{\mu} \qquad \text{(A19)}$$

where

$$K \equiv \frac{\rho c_A^2 \pi a_D^4}{\tau V} \qquad \text{(A20)}$$

Equation (A-19) gives the relation to be used for the value of χ in the subsequent relations employing this term.

A direct determination of the limit of the frequency parameter $H(\gamma, \mu)$ by letting γ and μ be zero in equation (A-11) cannot be obtained, since this results in an indeterminacy. Instead, the properties of the Bessel function series are utilized.

We first write $H(\gamma, \mu)$ as

$$H(\gamma,\mu) = \frac{J(\gamma,\mu)}{\mu^2 \Delta(\gamma,\mu)} \qquad \text{(A21)}$$

where

$$\left.\begin{aligned} J(\gamma,\mu) &= \frac{2}{\gamma} J_1(\gamma) - J_0(\mu) \\ \Delta(\gamma,\mu) &= \left[\left(J_0(\mu) - \frac{\gamma}{\mu} J(\gamma,\mu)\right)^2 + \left(\frac{\theta}{\mu}\right)^2 J^2(\gamma,\mu)\right]^{1/2} \qquad \text{(A22)} \\ \text{and} \quad \mu &= \frac{\omega a_D}{c} \;, \quad \gamma = \frac{\omega a_n}{c} \end{aligned}\right]$$

as before.

The limit of H (γ, μ) can then be obtained by finding the limit of J (γ, μ) and Δ (γ, μ) separately. Expanding J (γ, μ) in its series form, we have

$$\frac{J(\gamma,\mu)}{\mu^2} = \frac{1}{\mu^2}\left[\left(1 - \frac{\gamma^2}{2\cdot 4} + \frac{\gamma^4}{2\cdot 4^2\cdot 6} - \cdots + \right) - \left(1 - \frac{\mu^2}{4} + \frac{\mu^4}{2^2\cdot 4} - \cdots + \right)\right]$$

and dividing through by μ^2 and using only first terms in γ and μ we get

$$\left.\frac{J(\gamma,\mu)}{\mu^2}\right|_{w \to 0} = \frac{1}{4} - \frac{1}{8}\left(\frac{a_8}{a_0}\right)^2 \qquad \text{(A23)}$$

From equation (A-22) we see that the limit as $w \to 0$ of Δ (γ, μ) requires that the low frequency limit of $J_0(\mu)$, $\frac{\gamma}{\mu} J(\gamma,\mu)$ and $\left(\frac{\Theta}{\mu}\right)^2 J^2(\gamma,\mu)$ be found. From A-19, we can write

$$\frac{\gamma}{\mu} J(\gamma,\mu) = -\frac{K}{\mu^2} J(\gamma,\mu)$$

Therefore,

$$\lim_{w \to 0} \frac{\gamma}{\mu} J(\gamma,\mu) = \lim_{w \to 0} -\frac{K}{\mu^2} J(\gamma,\mu)$$

$$= -K\left[\frac{1}{4} - \frac{1}{8}\left(\frac{a_8}{a_0}\right)^2\right] \qquad \text{(A24)}$$

using the results of (A-23).

The third term in the relation for Δ (γ, μ) can be written as

$$\theta^2\left[\frac{J(\gamma,\mu)}{\mu^2}\right] J(\gamma,\mu)$$

where the term in brackets has already been evaluated. Θ is proportional

to the resistive part of z. This resistance is made up of the real part of the radiation impedance of the diaphragm which can be neglected at low frequencies and the real part of the thin film impedance directly behind the diaphragm. This latter resistance can be shown to be finite at low frequencies (Ref. 7). The term $J(\gamma, \mu)$ can be shown to be zero for low frequencies, as follows: From (A-22) we have

$$J(\gamma,\mu) = \frac{2}{\gamma} J_1(\gamma) - J_0(\mu) = J_2(\gamma) + J_0(\gamma) - J_0(\mu)$$

For $\omega = 0$, we get

$$\lim_{\omega \to 0} J(\gamma,\mu) = 0 + 1 - 1 = 0 \qquad \text{(A25)}$$

This result says that at low frequencies the resistive part of z plays no role in the average values of diaphragm displacement $\bar{\eta}$, regardless of its magnitude.

Substituting equations (A-23), (A-24) and (A-25) into (A-21), we find

$$\lim_{\omega \to 0} H(\gamma,\mu) = \frac{\frac{1}{4} - \frac{1}{8}\left(\frac{a_s}{a_p}\right)^2}{1 + K\left[\frac{1}{4} - \frac{1}{8}\left(\frac{a_s}{a_p}\right)^2\right]}$$

or, rearranging terms, we get

$$\lim_{\omega \to 0} H(\gamma,\mu) = \frac{\frac{2a_p^2 - a_s^2}{8a_p^2}}{1 + K\left[\frac{2a_p^2 - a_s^2}{8a_p^2}\right]} \qquad \text{(A26)}$$

Substituting into equation (A-17) we get the magnitude of the low frequency response of a condenser microphone.

$$M' = \frac{E_0(2a_p^2 - a_s^2)}{8sT} \cdot \frac{1}{1 + K\left(\frac{2a_p^2 - a_s^2}{8a_p^2}\right)} \qquad \text{(A27)}$$

The factor K accounts for the stiffness added to the mechanical impedance of the diaphragm by the small cavity behind it. From equation (A-20) we see that for a large value of diaphragm tension T relative to the volume stiffness, K is small and can be neglected. Under the condition that $K << 1$ and $a_B = a_D$ we see that

$$\underset{\substack{K<<1 \\ a_B = a_D}}{M'} = \frac{E_0 a_D^2}{8 s T} \tag{A28}$$

which is the more conventional relation for the low frequency sensitivity of a condenser microphone. The terms in parentheses in (A-27) accounts for the fact that the backplate and diaphragm radius are different. In fact, for maximum sensitivity, equation (A-27) requires that $a_B << a_D$. In this case, we get for M'

$$\underset{a_B << a_D}{M'} = \frac{E_0 a_D^2}{4 s T} \quad \frac{1}{1 + \frac{K}{4}} \tag{A29}$$

This result states that for the case when cavity stiffness can be neglected and hence $K << 1$ then the sensitivity of a condenser microphone of given radius and tension can be doubled by making its backplate radius small relative to its diaphragm radius. We caution that a limit is quickly reached, however, because the active capacity of the microphone becomes small and then shunt capacitances become more important and can result in signal losses.

B. Vibration Sensitivity

The relation between the "equivalent" sound pressure level, diaphragm mass and vibration acceleration amplitude can be derived quite simply with the use of Newton's second law. In terms of force per unit area or pressure (p) acting on the diaphragm and mass per unit area (ρ_s), Newton's second law can be expressed as

$$p = \rho_s a \tag{A30}$$

where a is the acceleration of the microphone diaphragm. Since the signal output from a condenser microphone is proportional to the diaphragm displacement, which is directly proportional to the acoustic pressure p acting uniformly on the diaphragm, the relation above says that there exists an acceleration "a" which will produce the same signal output as a pressure p. In terms of the sound pressure level (SPL) and (g), the acceleration due to gravity, we have

$$20 \log_{10} \frac{p}{p_{REF.}} = 20 \log_{10} \frac{\rho_s}{p_{REF.}} + 20 \log_{10} \frac{a}{g} \cdot g$$

letting $p_{REF.} = 2 \times 10^{-4}$ dyne/cm^2

$g = 980$ cm/sec^2

we get

$$SPL = 20 \log_{10} \rho_s + 20 \log_{10} \frac{a}{g} + 134 \quad db \qquad (A31)$$

The relation then expresses sound pressure level, diaphragm surface density and the vibration acceleration amplitude in "g" units.

For the A-6 microphone $\rho_s = 11.72 \times 10^{-3}$ gm/cm^2, hence for a 1 g acceleration amplitude the signal output produced by the microphone is equal to that produced by the calculated value of SPL from equation (A-31).

$$SPL = 20 \log 11.72 \times 10^{-3} + 134 \text{ db}$$

$$= -38.6 + 134 = 95.4 \text{ db}$$

Experience shows that the measured output for condenser microphones subjected to known accelerations agrees with the values calculated using equation (A-31).

C. Altitude Response of a Sealed Condenser Microphone

A sealed condenser microphone will undergo a loss in sensitivity due to an increase in the average distance between the diaphragm and backplate when subjected to an external increase in altitude or an external decrease in atmospheric pressure. The results of Section A of this appendix allows a theoretical calculation of this change in sensitivity. In the following discussion it is assumed that the tension on the diaphragm remains constant with increase in pressure differential across the diaphragm. Actually, this assumption may be violated for very high altitudes or large pressure differentials if the tension on the diaphragm is not sufficiently large to restrict the diaphragm displacements to small values. In other words, if the displacements due to pressure differential are not small, then the theory on which the discussion of Section A is founded does not hold here.

Using equation (A-27) we see that the ratio of the sensitivity of a microphone at sea level M_1' and at some altitude M_2' is given by

$$\frac{M_1'}{M_2'} = \frac{s_2}{s_1} \qquad \text{where}$$

s_1 and s_2 represents the average spacing between the microphone diaphragm and the backplate at the two conditions of altitude. We note here that in addition to the altitude pressure differential P_M acting on the diaphragm, there is an additional effective pressure P_E in the form of an electrostatic force which is due to the polarizing voltage on the microphone. This electrostatic force acts in opposition to the altitude induced force and account of this must be taken care of in the value of pressure in equation (A-10). This can be performed by letting the resultant pressure P in equation (A-10) equal to the sum of the two pressures, i.e. $P = P_M - P_E$ (A32)

If we now let s_o be the spacing between the microphone diaphragm and backplate when both P_M and P_E are zero, then it is seen that

$$\frac{M_1'}{M_2'} = \frac{s_2}{s_1} = \frac{s_o + \overline{\eta}_{P_M \neq 0}}{s_o + \overline{\eta}_{P_M = 0}} \tag{A33}$$

where

$$s_2 = s_o + \overline{\eta}_{P_M \neq 0}$$
$$s_1 = s_o + \overline{\eta}_{P_M = 0} \tag{A34}$$

and $\overline{\eta}_{P_M = 0}$ is the average diaphragm displacement at sea level and is due only to the electrostatic pressure P_E and $\overline{\eta}_{P_M \neq 0}$ is the resultant displacement at some altitude. Using the zero frequency limit of $H(\gamma, \mu)$ which is given by equation (A-26) and substituting into equation (A-10), we see that the magnitude of $\overline{\eta}$ is

$$\left| \overline{\eta} \right| = \frac{P\left(2a_o^2 - a_B^2\right)}{8T\left[1 + K\left(\frac{2a_o^2 - a_B^2}{8\, a_o^2}\right)\right]} \tag{A35}$$

where P is given by equation (A-32).

Using (A-35) in (A-33) gives

$$\frac{M_1'}{M_2'} = \frac{s_o + (P_M - P_E)\, B}{s_o - P_E\, B}$$
$$= 1 + \frac{P_M}{\frac{s_o}{B} - P_E} \tag{A36}$$

where $$B \equiv \frac{2a_0^2 - a_B^2}{8\tau\left[1 + K\left(\frac{2a_0^2 - a_B^2}{8a_0^2}\right)\right]} \qquad \text{(A37)}$$

and the other variables are as defined earlier. The term P_E has been included in the derivation for completeness. However, for most condenser microphones, and in particular for the A-6 microphones, it is small relative to s/B and hence can be neglected. With this in mind, it is clear from (A-36) that the change in sensitivity with altitude is small when $P_M << s_o/B$ which says that the tension on the microphone diaphragm must be large.

D. Dynamic Pressure Range

The dynamic pressure range for condenser microphone systems is generally bounded at lower sound pressure levels by system electrical noise and at higher sound pressure levels by the signal handling capability of the electronics associated with the microphone. The condenser microphone itself can be a problem at higher sound pressure levels if the average diaphragm displacement is not small relative to the equilibrium diaphragm-to-backplate spacing. The relation between average diaphragm displacement, $\bar{\eta}$, acoustic pressure p, and diaphragm tension τ at low frequencies, is given by equation (A-35), and is

$$\left|\bar{\eta}\right| = \frac{p(2a_0^2 - a_B^2)}{8\tau} \cdot \frac{1}{\left[1 + K\left(\frac{2a_0^2 - a_B^2}{8a_0^2}\right)\right]} \qquad \text{(A38)}$$

where we have neglected P_E since for the sound pressure levels of interest here it is much smaller than p. If we let s be the equilibrium diaphragm-to-backplate spacing, then the criterion we set is that $\frac{|\bar{\eta}|}{s} << 1$. From equation (A-38) we have therefore

$$p << \frac{8\tau s}{(2a_0^2 - a_B^2)}\left[1 + K\left(\frac{2a_0^2 - a_B^2}{8a_0^2}\right)\right] \qquad \text{(A39)}$$

Equation (A-39) gives the criterion for sound pressure p which will prevent distortion due to diaphragm displacement amplitude.

Supplying the parameters for the A-6 microphone, we get

$$p << 1.73 \times 10^6 \text{ dyne/cm}^2$$

or, in sound pressure level,

$$SPL << 199 \text{ db}$$

Using the criterion that $\bar{y}/s = 1/10$, we see that the upper limit of linear diaphragm displacement occurs at a sound pressure level of about 180 db. We note that this limit is about 10 db below the target specification of 190 db.

Equation (A-39) suggests three alternatives to increase the upper SPL limit. The first is to increase the value of τ, and therefore the diaphragm stress. However, reference to figure 3 shows that the potential increase in maximum SPL is only about 1.0 db since the diaphragm stress can be increased from 150,000 psi to 170,000 psi while still maintaining the 600°F capability. Increasing the yield strength beyond 170,000 psi decreases diaphragm temperature exposure capability to less than 600°F, which is not desirable. The gain in maximum SPL of only 1.0 db did not warrant a decrease in temperature exposure capability from 800°F to 600°F, hence this alternative seemed undesirable and was not utilized.

The second alternative is to increase the value of s, the diaphragm-backplate spacing, which again decreases the microphone sensitivity. We note that this would also have the advantage of decreasing loss in microphone sensitivity versus pressure differential or altitude, as is shown in an earlier section. A disadvantage of this alternative is that higher diaphragm temperatures would result because of the significant increase in heat flow resistance between diaphragm and backplate.

The third alternative, of course, is to increase the diaphragm thickness, thus decreasing the diaphragm motion. Attendant reductions in the sensitivity variations with temperature and pressure would be advantages. The point is that any microphone, including the condenser type, has a limited range between the threshold noise and a specified limit of distortion. It is an extremely great range and it can be placed to suit the exposure conditions.

REFERENCES

1. "Microphone for the Measurement of Aerodynamic Pressure Fluctuations," Western Electro-Acoustic Laboratory, Inc., Final Report, 2 May 1963, Contract AF33(616)-4331.

3. Veneklasen, Paul S., "Instrumentation for the Measurement of Sound Pressure Level with the Western Electric 640AA Condenser Microphone," JASA 20, 807 (1948).

4. Lin, C. C., Turbulent Flows and Heat Transfer, Princeton University Press, 1959.

5. Morse, P. M., Vibration and Sound, McGraw-Hill Book Co., 1948.

6. Bowman, Frank, Introduction to Bessel Functions, Page 93, Dover Publications, Inc.

7. Crandall, Irving B., Theory of Vibration Systems and Sound, Page 28, D. Van Nostrand Co., Inc., 1926.

8. Olson, Harry F., Elements of Acoustical Engineering, D. Van Nostrand Co., Inc.

UNCLASSIFIED

Security Classification

DOCUMENT CONTROL DATA - R&D

(Security classification of title, body of abstract and indexing annotation must be entered when the overall report is classified)

1. ORIGINATING ACTIVITY (Corporate author)	2a. REPORT SECURITY CLASSIFICATION
Western Electro-Acoustic Laboratory, Inc. 2222 South Barrington Avenue Los Angeles, California 90064	UNCLASSIFIED 2b. GROUP N/A

3. REPORT TITLE

Microphone System for the Measurement of Boundary Layer Pressure Fluctuations

4. DESCRIPTIVE NOTES (Type of report and inclusive dates)

Final Report

5. AUTHOR(S) (Last name, first name, initial)

Ortega, Jose C.

6. REPORT DATE	7a. TOTAL NO. OF PAGES	7b. NO. OF REFS
January 1967	82	8

8a. CONTRACT OR GRANT NO.	9a. ORIGINATOR'S REPORT NUMBER(S)
AF33(615)-2544 b. PROJECT NO. 1472 c. Task 147203 d.	AFFDL-TR-66-196 9b. OTHER REPORT NO(S) (Any other numbers that may be assigned this report) None

10. AVAILABILITY/LIMITATION NOTICES

This document is subject to special export controls and each transmittal to foreign nationals may be made only with prior approval of AFFDL (FDD).

11. SUPPLEMENTARY NOTES	12. SPONSORING MILITARY ACTIVITY
None	Air Force Flight Dynamics Laboratory (FDDS) Wright-Patterson AFB, Ohio 45433

13. ABSTRACT

This report presents a description of a condenser microphone system developed for use in the measurement of boundary layer pressure fluctuations. Prime consideration in the design of the transducer of the system was the requirement for operation in abnormal environments, with emphasis on high temperature. Calibrations are described in the report which show that the Western Electro-Acoustic Laboratory A-6 condenser microphone can operate at diaphragm temperatures to 800°F.

Measurements utilizing an electrical analog of the microphone thermal characteristics and flat plate boundary layer theory show that an 800°F upper limit for the transducer would satisfy nearly all conceivable uses of the system in practice. For example, for a "flight" condition of Mach 4.2 at sea level, where the recovery temperature would be 1600°F, the diaphragm temperature would reach 800°F. This same speed at 40,000 ft. would result in a diaphragm temperature of 300°F. A speed of Mach 6.9 would be required to produce an 800°F diaphragm temperature at 40,000 ft. These flight conditions are extreme for present day vehicles, including re-entry vehicles, hence the transducer can be used over a very large range of altitudes and Mach numbers.

This report presents the methods and results of calibration, as well as some of the shortcomings of the system.

DD FORM 1 JAN 64 1473

UNCLASSIFIED

Security Classification

UNCLASSIFIED

Security Classification

14. KEY WORDS	LINK A		LINK B		LINK C	
	ROLE	WT	ROLE	WT	ROLE	WT
Boundary layer pressure fluctuations, Weal Modal A-6 Microphone System, Extreme High-temperature environment, Combined environment testing.						

INSTRUCTIONS

1. ORIGINATING ACTIVITY: Enter the name and address of the contractor, subcontractor, grantee, Department of Defense activity or other organization *(corporate author)* issuing the report.

2*a*. REPORT SECURITY CLASSIFICATION: Enter the overall security classification of the report. Indicate whether "Restricted Data" is included. Marking is to be in accordance with appropriate security regulations.

2*b*. GROUP: Automatic downgrading is specified in DoD Directive 5200.10 and Armed Forces Industrial Manual. Enter the group number. Also, when applicable, show that optional markings have been used for Group 3 and Group 4 as authorized.

3. REPORT TITLE: Enter the complete report title in all capital letters. Titles in all cases should be unclassified. If a meaningful title cannot be selected without classification, show title classification in all capitals in parenthesis immediately following the title.

4. DESCRIPTIVE NOTES: If appropriate, enter the type of report, e.g., interim, progress, summary, annual, or final. Give the inclusive dates when a specific reporting period is covered.

5. AUTHOR(S): Enter the name(s) of author(s) as shown on or in the report. Enter last name, first name, middle initial. If military, show rank and branch of service. The name of the principal author is an absolute minimum requirement.

6. REPORT DATE: Enter the date of the report as day, month, year; or month, year. If more than one date appears on the report, use date of publication.

7*a*. TOTAL NUMBER OF PAGES: The total page count should follow normal pagination procedures, i.e., enter the number of pages containing information.

7*b*. NUMBER OF REFERENCES: Enter the total number of references cited in the report.

8*a*. CONTRACT OR GRANT NUMBER: If appropriate, enter the applicable number of the contract or grant under which the report was written.

8*b*, 8*c*, & 8*d*. PROJECT NUMBER: Enter the appropriate military department identification, such as project number, subproject number, system numbers, task number, etc.

9*a*. ORIGINATOR'S REPORT NUMBER(S): Enter the official report number by which the document will be identified and controlled by the originating activity. This number must be unique to this report.

9*b*. OTHER REPORT NUMBER(S): If the report has been assigned any other report numbers *(either by the originator or by the sponsor)*, also enter this number(s).

10. AVAILABILITY/LIMITATION NOTICES: Enter any limitations on further dissemination of the report, other than those imposed by security classification, using standard statements such as:

(1) "Qualified requesters may obtain copies of this report from DDC."

(2) "Foreign announcement and dissemination of this report by DDC is not authorized."

(3) "U. S. Government agencies may obtain copies of this report directly from DDC. Other qualified DDC users shall request through

_____."

(4) "U. S. military agencies may obtain copies of this report directly from DDC. Other qualified users shall request through

_____."

(5) "All distribution of this report is controlled. Qualified DDC users shall request through

_____."

If the report has been furnished to the Office of Technical Services, Department of Commerce, for sale to the public, indicate this fact and enter the price, if known.

11. SUPPLEMENTARY NOTES: Use for additional explanatory notes.

12. SPONSORING MILITARY ACTIVITY: Enter the name of the departmental project office or laboratory sponsoring *(paying for)* the research and development. Include address.

13. ABSTRACT: Enter an abstract giving a brief and factual summary of the document indicative of the report, even though it may also appear elsewhere in the body of the technical report. If additional space is required, a continuation sheet shall be attached.

It is highly desirable that the abstract of classified reports be unclassified. Each paragraph of the abstract shall end with an indication of the military security classification of the information in the paragraph, represented as *(TS)*, *(S)*, *(C)*, or *(U)*.

There is no limitation on the length of the abstract. However, the suggested length is from 150 to 225 words.

14. KEY WORDS: Key words are technically meaningful terms or short phrases that characterize a report and may be used as index entries for cataloging the report. Key words must be selected so that no security classification is required. Identifiers, such as equipment model designation, trade name, military project code name, geographic location, may be used as key words but will be followed by an indication of technical context. The assignment of links, rules, and weights is optional.

UNCLASSIFIED

Security Classification